AWARD NUMBER: W81XWH-14-1-0403
PC130359

TITLE: The Roles of the Bone Marrow Microenvironment in Controlling Tumor Dormancy

PRINCIPAL INVESTIGATOR: Yusuke Shiozawa, M.D., Ph.D.

CONTRACTING ORGANIZATION: Wake Forest University
Winston Salem, NC 27157

REPORT DATE: May 2019

TYPE OF REPORT: Final report

PREPARED FOR: U.S. Army Medical Research and Materiel Command
Fort Detrick, Maryland 21702-5012

REPORT DOCUMENTATION PAGE

Form Approved
OMB No. 0704-0188

1. REPORT DATE	2. REPORT TYPE	3. DATES COVERED
May 2019	Final	8SEP2014 - 28FEB2019

4. TITLE AND SUBTITLE
The Roles of the Bone Marrow Microenvironment in Controlling Tumor Dormancy

5a. CONTRACT NUMBER

5b. GRANT NUMBER
W81XWH-14-1-0403

5c. PROGRAM ELEMENT NUMBER

6. AUTHOR(S)
Yusuke Shiozawa, MD, PhD

E-Mail: yshiozaw@wakehealth.edu

5d. PROJECT NUMBER

5e. TASK NUMBER

5f. WORK UNIT NUMBER

7. PERFORMING ORGANIZATION NAME(S) AND ADDRESS(ES)
Wake Forest University Health Sciences
Medical Center Blvd.
Winston-Salem NC 27157

8. PERFORMING ORGANIZATION REPORT NUMBER

9. SPONSORING / MONITORING AGENCY NAME(S) AND ADDRESS(ES)
U.S. Army Medical Research and Materiel Command
Fort Detrick, Maryland 21702-5012

10. SPONSOR/MONITOR'S ACRONYM(S)

11. SPONSOR/MONITOR'S REPORT NUMBER(S)

12. DISTRIBUTION / AVAILABILITY STATEMENT
Approved for Public Release; Distribution Unlimited

13. SUPPLEMENTARY NOTES

14. ABSTRACT

The purpose of this study is to identify the mechanisms whereby the bone marrow microenvironment is involved in the regulation of tumor dormancy. Aim1 will identify and explore how disseminated tumor cells (DTCs) stay dormant for long periods of time. We postulate that DTCs drive the bone marrow niche into dormancy. Aim2 will determine how DTCs escape dormancy, consequently rendering them more susceptible to the chemotherapy.

During this period, we found that a slow-growing prostate cancer (PCa) may contribute to the maintenance of osteoblastic niche dormancy *in vitro*. In addition, we observed that a fast-growing osteoblast may have ability to induce bone metastatic PCa growth, and that a fast-growing osteoblast may enhance susceptibility of bone metastatic PCa to chemotherapy.

15. SUBJECT TERMS
Prostate Cancer; Bone metastasis; Disseminated tumor cells; Bone marrow microenvironment; Tumor dormancy; GAS6; BMP2

16. SECURITY CLASSIFICATION OF:			17. LIMITATION OF ABSTRACT	18. NUMBER OF PAGES	19a. NAME OF RESPONSIBLE PERSON
a. REPORT	b. ABSTRACT	c. THIS PAGE			USAMRMC
Unclassified	Unclassified	Unclassified	Unclassified	32	19b. TELEPHONE NUMBER *(include area code)*

Table of Contents

1. INTRODUCTION:

Despite improvements in treatments for primary prostate cancer (**PCa**), bone metastasis remains a major cause of death in PCa patients. Several studies have shown that disseminated tumor cells (**DTCs**) shed from a primary tumor may lie dormant in distant tissues for long periods of time, retaining the potential for activation resulting in metastatic growth. Understanding the underlying mechanisms of metastasis is therefore crucial for effective treatment of this disease. Bone marrow has been well established as a regulatory site for hematopoietic function. In the marrow, hematopoietic stem cells (**HSCs**) are believed to localize to a specific microenvironment, the "niche", where they reside in a dormant state. Likewise, growing evidence has suggested that disseminated PCa also resides within the marrow niche. In fact, disseminated PCa uses similar mechanisms as HSCs in order to gain access to the marrow microenvironment, and DTCs target and displace HSCs, establishing metastatic foci within the hematopoietic niche. As a result, these cells parasitize the niche to become dormant, utilizing the mechanisms that keep HSCs in a dormant state. Although bone marrow is known as a fertile microenvironment ("soil") for metastatic tumor cells ("seed"), little is known about how dormancy is established or what leads to re-activation of the dormant cells. Therefore, we hypothesize that **once DTCs become dormant within the bone marrow niche, they stay dormant by stimulating the niche to remain dormant, and eventually escape from dormancy when the niche matures.**

To address our hypothesis the following aims are proposed:
Aim1: Determine the mechanisms whereby DTCs control the dormancy of the niche cells.
Sub hypothesis: DTCs drive the niche into dormancy via GAS6 signaling.
Aim2: Determine if the differentiation of the niche cells triggers the regrowth of DTCs.
Sub hypothesis: Dormant DTCs exit from dormancy when the niche is differentiated via BMP2 signaling.

The proposed studies will provide significant insight into the mechanisms whereby the bone marrow microenvironment is involved in regulation of tumor dormancy. Aim 1 allows us to identify and explore how DTCs stay dormant for long periods of time. We postulate that DTCs drive the bone marrow niche into dormancy through the GAS6 pathway. Aim2 will determine how DTCs escape dormancy, consequently rendering them more susceptible to the chemotherapy. Results from this work will lead to a greater understanding of niche aging effects on metastatic growth, and could result in valuable new treatment approaches.

2. KEYWORDS:

Prostate Cancer; Bone metastasis; Disseminated tumor cells; Bone marrow microenvironment;
Tumor dormancy; GAS6; BMP2

3. ACCOMPLISHMENTS:

What were the major goals and objectives of the project?

The goal of this project is to understand the mechanisms of tumor dormancy and metastatic outgrowth of disseminated prostate cancer within the bone marrow microenvironment.

Task 1: Complete the grant transfer from University of Michigan to Wake Forest School of Medicine.

Months 1-3.

- Upon arrival at Wake Forest School of Medicine, the PI will seek to obtain the necessary approvals (IACUC, IRB, IBC) to complete the grant transfer, and then will initiate the proposed research as soon as possible (**Months 1-3**).

Task 2: Determine the mechanisms whereby DTCs control the dormancy of the niche cells.

Months 4-18.

- To determine the effects of GAS6 on the dormancy of niche cells *in vitro*, co-culture of bone marrow stromal cells (**BMSCs**) (pre-stained with DiD fluorescent dye) with either GAS6-downregulated PCa cells (**PCa^{shGAS6}**) or control PCa (**PCa^{Control}**) will be performed. At the termination of experiments, BMSCs will be harvested, and the retention of DiD dye will be measured with FACS (**Months 4-7**).

  To further characterize the difference, gene and protein expression of proliferation markers and cell cycle status will be analyzed using those isolated BMSCs (**Months 7-9**).

- To determine the effects of GAS6 on the dormancy of niche cells *in vivo*, we will perform a vertebral body implant (vossicle) experiment. We will implant BrdU-incorporated vossicles directly injected with PCa^{shGAS6} or PCa^{Control} into immunocompromized mice, and then will determine the effects of GAS6 on the dormancy of the microenvironment by immunohistochemistry for BrdU (**Months 9-14**).

  Additionally, using immunohistochemistry we will also visualize co-localization of PCa cells with the dormant microenvironment cells using these vossicles (**Months 14-19**).

Task 3: Determine if the differentiation of the niche cells triggers the regrowth of DTCs.

Months 19-36.

- To determine if the differentiation of the niche following exogenous BMP2 treatment stimulates the regrowth of DTCs *in vitro*, co-culture of BMSCs with G1-Red and SG2M-Cyan co-infected PCa cells will be performed. The differentiation of the niche, and the dormancy, proliferation, and cell cycle status of PCa cells after treatment with recombinant mouse (**rm**) BMP2 will be analyzed (**Months 19-22**).

- To determine if the differentiation of the niche following the exogenous BMP2 treatment stimulates the regrowth of DTCs *in vivo*, we will implant vossicles directly injected with G1-Red and SG2M-Cyan co-infected PCa cells into immunocompromized mice. The differentiation of the niche, and the dormancy, proliferation, and cell cycle status of PCa cells after treatment with rm BMP2 will be analyzed (**Months 22-26**).

- To determine whether BMP2 expressed by DTCs is crucial for metastatic progression *in vitro*, co-culture of BMSCs with BMP2-downregulated PCa (**PCa^{shBMP2}**), upregulated PCa (**PCa^{BMP2OE}**), or control PCa (**PCa^{Control}**) will be performed. Thereafter, the differentiation of the niche, and the dormancy, proliferation, and cell cycle status of PCa cells will be analyzed (**Months 27-30**)

- To determine whether BMP2 expressed by DTCs is crucial for metastatic progression *in vivo*, we will implant vossicles directly injected with PCa^{shBMP2}, PCa^{BMP2OE}, or PCa^{Control}. Thereafter, the differentiation of the niche, and the dormancy, proliferation, and cell cycle status of PCa cells will be analyzed (**Months 31-36**).

What was accomplished under these goals?

(~2017)

The Award transfer.

As of 03/01/15, thanks to receiving this Idea Development Award for Young Investigators, the PI, Dr. Yusuke Shiozawa started an independent faculty job as an Assistant Professor at Wake Forest School of Medicine. Upon his arrival at Wake Forest School of Medicine, the PI obtained the necessary institutional approvals (IACUC, IRB, IBC) and submitted the grant transfer request (06/11/2015) to gain approval from the Department of Defense for a transfer of the award from the University of Michigan to Wake Forest School of Medicine. As of 07/01/16, a transfer of the award from the University of Michigan to Wake Forest School of Medicine was completed.

The development of a mouse model to measure tumor growth and bone remodeling.

We established an innovative and powerful mouse model to measure tumor growth and bone remodeling within the same animal. For this experiment, PCa cells (DU145) were inoculated intrafemorally into severe combined immunodeficient (**SCID**) mice to establish bone metastases. Thereafter, we measured changes in tumor growth [bioluminescent imaging (**BLI**), immunohistochemistry (**IHC**)] and bone remodeling (microCT, IHC). Using this strategy, we found (i) tumor growth by BLI, (ii) tumor burden in the marrow by histology, and decreased bone volume density and connective density in tumor-burdened mice on microCT.

The neuropeptide CGRP expressed by sensory neurons around bone influences PCa proliferation through CRLR/JNK pathway.

We found that calcitonin-gene related peptide (**CGRP**) enhances proliferation of PCa cells *in vitro*. PCa patients with metastases express higher levels of CGRP receptor Calcitonin receptor like receptor (**CRLR**) (gene name

CALCRL), compared to PCa patients without metastases. Additionally, CGRP activates JNK in PCa.

The fast growing less differentiated osteoblasts may contribute more to tumor growth, compared to mature osteoblasts *in vitro*.

We found the mandible osteoblasts (**MaOB**) to be much more proliferative than the hind limb osteoblasts (**HLOB**). As expected, both osteoblasts express osteoblast differentiation markers osteocalcin and osteopontin. Finally, when PCa cells were cocultured with these osteoblasts, we found that both PC3 and DU145 grew significantly faster in coculture with MaOB compared to HLOB, suggesting that a less proliferative osteoblast may contribute more to tumor dormancy than a fast-growing osteoblast.

(2017-2018)

No Cost Extension.

As of 06/28/18, a no cost extension of this project through 2/29/19 was approved.

Bone morphogenetic protein (BMP)7 derived from dormant PCa induces osteoblast dormancy.

We segregated fast-growing and slow-growing (or dormant) PCa cells using the membrane-bound dye DiD and found that slow-growing PCa cells express higher levels of BMP7 mRNA than fast-growing PCa cells. Although we originally hypothesized that GAS6 derived from PCa cells controls niche dormancy, we did not see a difference in GAS6 mRNA levels between fast-growing and slow-growing PCa cells. We also observed that BMP7 expression in PCa was upregulated when cocultured with osteoblasts *in vitro*. Additionally, we found that BMP7 inhibits the proliferation of osteoblasts, but had no effect on the proliferation of PCa cells, and that slow-growing PCa cells support the maintenance of osteoblast dormancy, compared to fast-growing PCa cells, when PCa cells are co-cultured with osteoblasts.

Fast-growing osteoblasts have greater mineralization activity compared to less proliferative osteoblasts both *in vitro* and *in vivo.*

We found that fast-growing MaOBs form more mineralized bone matrix *in vitro* and calcified bone *in vivo*, compared to slow-growing HLOBs, and that MaOBs express less stem cell factor (SCF) than HLOBs.

(2018-2019)

Dormant PCa supports the maintenance of osteoblast quiescence longitudinally *in vitro*.

During the last report period, we observed that DiD high, slow-glowing PCa cells can support the maintenance of osteoblast quiescence, compared to DiD low, fast-glowing PCa cells. On top of this, the proliferation of osteoblasts was measured by flow cytometry using a fluorescent retention method. The data was informative, but the use of the fluorescent retention method is limiting in that it requires the collection of large numbers of slow-growing and fast-growing PCa cells, and makes longitudinal studies difficult as the readout requires termination of the experiment prior to flow cytometric analyses. Therefore, to better obtain large numbers of slow-growing and fast-growing PCa cells, we treated PCa cells (PC3 and DU145) with Mitomycin C, which is

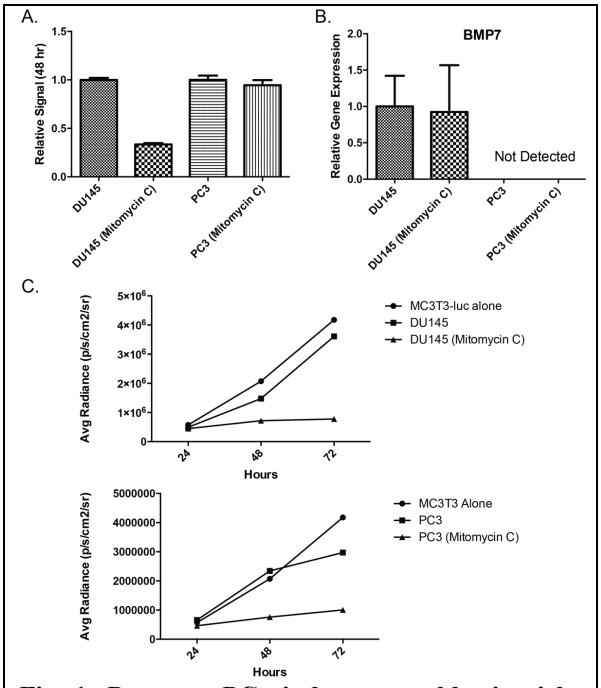

Fig. 1: Dormant PCa induces osteoblastic niche dormancy.
(**A**) Luciferase-expressing PCa cells (DU145, PC3) were treated with 10 μg/mL Mitomycin C to induce cell cycle arrest for 30 min. Growth of PCa cells was measured by bioluminescent imaging (BLI) 48 hr after treatment. (**B**) BMP7 mRNA levels in PCa cells recovered from (**A**) were measured by qPCR. (**C**) PCa cells were treated with or without 10 μg/mL Mitomycin C to induce cell cycle arrest for 30 min and 24 hr later, Luciferase-expressing MC3T3-E1 cells were cultured directly on top. Proliferation of MC3T3-E1 cells was tracked using BLI over a 72 hr time-course.

known to induce cell cycle arrest by inhibiting DNA synthesis. As expected, Mitomycin C inhibited the proliferation

of PCa cells, while the proliferation of vehicle-treated control PCa cells

increased (**Fig. 1A**). Although we saw higher levels of BMP7 mRNA in DiD high, slow-growing PCa cells than fast-growing PCa cells during the last report period, we found that BMP7 mRNA in PCa cells was extremely low, and not at all enhanced by Mitomycin C treatment and growth arrest (**Fig. 1B**). Next, to perform a longitudinal follow-up of osteoblast proliferation, we developed luciferase-positive murine osteoblast cell line MCMT3-E1 cells. Thereafter, luciferase-expressing MC3T3-E1 cells were co-cultured with either Mitomycin C treated (dormant) PCa cells or vehicle treated (growing) PCa cells. As previously demonstrated, the proliferation of osteoblasts slowed when they were co-cultured with PCa cells, compared to MC3T3-E1 cells alone (**Fig. 1C**). Interestingly, the proliferation of osteoblasts was further inhibited when they were co-cultured with Mitomycin C treated PCa cells and this was observed in a longitudinal manner (**Fig. 1C**).

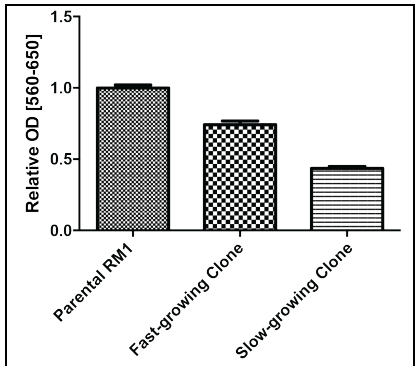

Fig. 2: Establishment of fast-growing and slow-growing PCa clones.
Slow-growing and fast-growing murine PCa cell line RM-1 cells were established using the limiting dilution cell cloning method. MTT assay was used to validate differential clone proliferation rates after 72 hr in culture.

To further address the effects of PCa proliferation on osteoblastic niche quiescence, we established "slow-growing" and "fast-growing" clones of the murine PCa cell line RM-1 using the limiting dilution cell cloning method since the cell growth arrest mediated by agents like Mitomycin C is not usually permanent. After the slow-growing and fast-growing RM-1 clones were established, their proliferation was measured *in vitro* (**Fig. 2**). Thereafter, these slow-growing and fast-growing murine RM-1 cells were inoculated into the femurs of mice. However, unexpectedly both *in vitro* slow-growing and fast-growing RM-1 cells grew similarly *in vivo* (Data not shown). Moreover, the tumor-inoculated bones collected from these mice were extremely osteolytic, which made the comparison of osteoblast proliferation very difficult (Data not shown). Therefore, our current focus is on the development of more reliable tumor dormancy mouse models to overcome these difficulties.

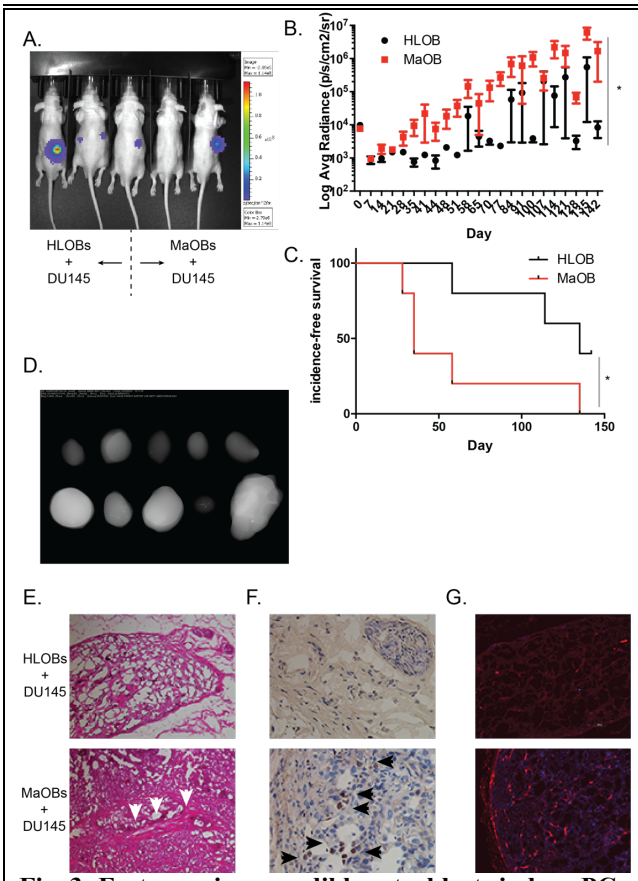

Fig. 3: Fast-growing mandible osteoblasts induce PCa growth in the bone.
HLOBs and MaOBs were seeded in gelatin scaffolds (ossicles) with DU145 cells and implanted into recipient mice (Left flank: HLOBs + DU145, Right flank: MaOBs + DU145). The growth of PCa cells within the implants was tracked by BLI for 142 days. (**A**) Representative BLI image at day 142. (**B**) Quantification of (A). (Two-way ANOVA). (**C**) Incidence-free survival of (**A**) (Gehan-Breslow-Wilcoxon Test) Mean ± SEM, $^{*}p \leq 0.05$. At day 142, the mice were euthanized, ossicles dissected, and (**D**) calcification was assessed by X-ray, and (**E**) bone formation (H&E, white arrows: bone nodules), (**F**) proliferation of PCa in implants (BRDU staining, black arrows: proliferating cells), and (**G**) vascularization (endomucin staining) were assessed by immunohistochemical analyses.

Fast-growing osteoblasts induce greater PCa growth *in vivo* and enhance the susceptibility of PCa cells to chemotherapy *in vitro*, compared to less proliferative osteoblasts

During the last report period, we found that fast-growing MaOBs form more bone both *in vitro* and *in vivo*, compared to slow-growing HLOBs. Therefore, to determine the effects of proliferation of osteoblasts on tumor growth in the bone, DU145 cells were co-implanted with either MaOBs or HLOBs into the flanks of immunodeficient mice. Intriguingly, DU145 cells co-implanted with MaOBs grew tumors sooner and faster than those with co-implanted with HLOBs (**Fig. 3A-C**). As previously reported, MaOBs formed more calcified bone than HLOBs, even though they were co-implanted with PCa cells (**Fig. 3D**). Immunohistochemical analyses demonstrated that the implants of MaOBs and DU145 cells showed more osteoblastic activities (**Fig. 3E**), more PCa proliferation (**Fig. 3F**), and more vascularization (**Fig. 3G**), compared to those of HLOBs and DU145 cells.

We also sought to determine the effects of osteoblast proliferation on susceptibility of PCa cells to chemotherapies since these cytotoxic agents target fast growing cells. To address this question, MaOBs or HLOBs were co-cultured with DU145 cells and then treated with Docetaxel. Interestingly, DU145 cells were more susceptible to Docetaxel when co-cultured with MaOBs than HLOBs (**Fig. 4A**). However, the co-culture between osteoblasts and PCa cells did not protect osteoblasts from the cytotoxicity of Docetaxel (**Fig. 4B**). Although we hypothesized that BMP2 treatments prior to chemotherapy can enhance susceptibility of PCa cells to chemotherapy, we previously failed to induce osteoblastic proliferation with BMP2. Therefore, our future experiments are to identify the agents that alter osteoblastic proliferation and test whether priming osteoblasts with these potential agents can enhance susceptibility of PCa to chemotherapies.

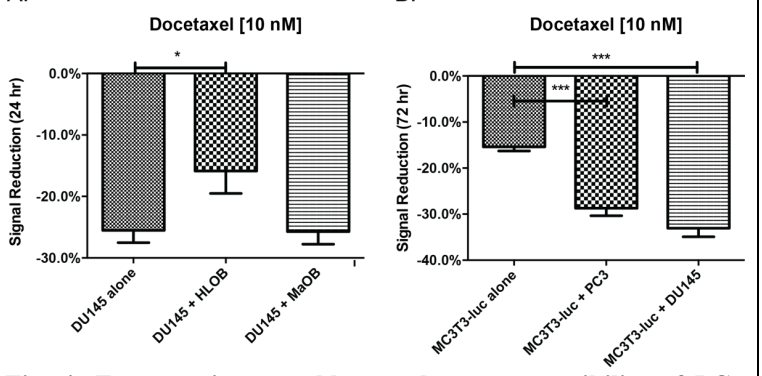

Fig. 4: Fast-growing osteoblasts enhance susceptibility of PCa cells to chemotherapy.
(**A**) Luciferase-expressing DU145 cells were co-cultured with HLOBs and MaOBs, and then treated with 10 nM Docetaxel for 24 hr. After, the reduction in BLI signal was compared against control co-cultures (without Docetaxel treatment). (**B**) Luciferase-expressing MC3T3-E1 cells were co-cultured with PCa cells (DU145, PC3), and then treated with 10 nM Docetaxel for 72 hr. After, the reduction in BLI signal was compared against control co-cultures (without Docetaxel treatment). (One-way ANOVA, Tukey's multiple comparison). Mean ± SEM, $^{*}p \leq 0.05$, $^{***}p \leq 0.001$.

What opportunities for training and professional development did the project provide?

(~2017)

Thanks to receiving an Idea Development Award for Young Investigators, the PI obtained independent status at Wake Forest School of Medicine with lab space, office space, and start-up costs provided.

Thanks to the Department of Defense, the PI attended IMPaCT Young Investigator Meeting, Baltimore, MD, USA, August 4-5, 2016.

The PI was chosen for the 2016-2018 cohort of the Wake Forest Clinical and Translational Science Institute's Translational Scholar Academy, which supports the scientific and career development of early-stage investigators.

The PI was invited to attend The U.S. Bone and Joint Initiative (USBJI) and Bone and Joint Canada (BJC) Young Investigator Initiative Program (Toronto, Canada) on 11/10/17-11/12-17.

(2017-2018)

The PI was invited to give a seminar at Jikei University School of Medicine (Tokyo, Japan) on October 11, 2017.

(2018-2019)

The PI was invited back to attend The U.S. Bone and Joint Initiative (USBJI) and Bone and Joint Canada (BJC) Young Investigator Initiative Program (Rosemont, IL) on 04/26/19-04/28/19.

How were the results disseminated to communities of interest?

There is nothing to report at this time.

What do you plan to do during the next reporting period to accomplish the goals and objectives?

There is nothing to report at this time.

4. IMPACT:

What was the impact on the development of the principal discipline(s) of the project?

(~2017)

We developed an innovative and powerful mouse models that enable us to measure within the same animal: (i) the growth of bone metastatic PCa and (ii) bone remodeling.

We developed a new and creative tool (mandible vs. hind limb osteoblast) to test the hypothesis that active osteoblasts enhance the re-growth of cancer in the bone.

Using this technique, we found that a fast-growing less differentiated osteoblast may contribute to growth of bone metastatic prostate cancer.

(2017-2018)

We found that PCa cells do not rest passively in their niche. Instead, they directly participate in niche activities by maintaining osteoblastic niche dormancy.

We found that fast-growing osteoblasts form more bone and express less stem cell factor (SCF), suggesting that increased osteoblast activity and loss of SCF may contribute to the outgrowth of bone metastatic PCa.

(2018-2019)

We found that slow-growing PCa cells are involved in the maintenance of dormancy of osteoblastic niche in a longitudinal manner *in vitro*.

We found that fast-growing osteoblasts induce greater PCa growth *in vivo*, compared to slow-growing osteoblasts, and that fast-growing osteoblasts also enhance susceptibility of PCa to chemotherapy, suggesting that increased osteoblast activity prior to chemotherapy may be a promising new treatment strategy for bone metastatic PCa.

What was the impact on other disciplines?

There is nothing to report at this time.

What was the impact on technology transfer?

There is nothing to report at this time.

What was the impact on society beyond science and technology?

There is nothing to report at this time.

5. CHANGES/PROBLEMS:

Changes in approach and reasons for change

Nothing to report.

Actual or anticipated problems or delays and actions or plans to resolve them

Nothing to report.

Changes that have a significant impact on expenditures

Nothing to report.

Significant changes in use or care of human subjects, vertebrate animals, biohazards, and/or select agents

Nothing to report.

6. PRODUCTS:

Publications, conference papers, and presentations

Journal Publications

Peer reviewed journal

(~2017)

1. Seib FP, Berry JE, **Shiozawa Y**, Taichman RS, Kaplan DL. Tissue engineering a surrogate niche for metastatic cancer cells. **Biomaterials**. 2015;51:313-9. PMID: 25771021. PMCID: PMC4367489.
   Status of Publication: Published
   Acknowledgement of federal support: Yes

2. Zalucha JL, Jung Y, Joseph J, Wang J, Berry JE, **Shiozawa Y**, Taichman RS. The Role of Osteoclasts in Early Dissemination of Prostate Cancer Tumor Cells. **J Cancer Stem Cell Res**. 2015;3:e1005. PMID: 26097863. PMCID: PMC4469294.
   Status of Publication: Published
   Acknowledgement of federal support: Yes

3. **Shiozawa Y**, Berry JE, Eber MR, Jung Y, Yumoto K, Cackowski FC, Yoon HJ, Parsana P, Mehra R, Wang J, McGee S, Lee E, Nagrath S, Pienta KJ, Taichman RS. The Marrow Niche Controls The Cancer Stem Cell Phenotype Of Disseminated Prostate Cancer. **Oncotarget**. In Press. PMID: 27172799. PMCID: PMC5173053.
   Status of Publication: Published
   Acknowledgement of federal support: Yes

4. Sharma S, Xing F, Liu Y, Wu K, Said N, Pochampally R, **Shiozawa Y**, Lin HK, Balaji KC, Watabe K. Secreted Protein Acidic and Rich in Cysteine (SPARC) Mediates Metastatic Dormancy of Prostate Cancer in the Bone. **J Biol Chem**. 2016;291:19351-63. PMID: 27422817. PMCID: PCM5016675.
   Status of Publication: Published
   Acknowledgement of federal support: No

5. Cackowski F, Eber MR, Rhee J, Decker A, Yumoto K, Berry JE, Lee E, **Shiozawa Y**, Jung Y, Aguirre-Ghiso JA, Taichman RS. Mer Tyrosine Kinase Regulates Disseminated Prostate Cancer Cellular Dormancy. **J Cell Biochem**. 2017;118:891-902. PMID: 27753136. PMCID: PMC5296338.
   Status of Publication: Published
   Acknowledgement of federal support: Yes

6. Kast RE, Skuli N, Cos S, Karpel-Massler G, **Shiozawa Y**, Goshen R, Halatsch ME. The ABC7 regimen: a new approach to metastatic breast cancer using seven common drugs to inhibit

epithelial-to-mesenchymal transition and augment capecitabine efficacy. **Breast Cancer (Dove Med Press)**. 2017;9:495-514. PMID: 28744157. PMCID: PMC5513700
Status of Publication: Published
Acknowledgement of federal support: Yes

(2017-2018)

7. Park SH, Eber MR, Tsuzuki S, Booker ME, Sunil AG, Widner DB, Parker RA, Peters CM, **Shiozawa Y**. Adeno-associated virus serotype rh10 is a useful gene transfer vector for sensory nerves that innervate bone in immunodeficient mice. **Sci Rep**. 2017;7:17428. PMID: 29233995. PMCID: PMC5727257.
Status of Publication: Published
Acknowledgement of federal support: Yes

- **Selected as Papers of the Week (9 Dec 2017- 15 Dec 2017) by Pain Research Forum**

(2018-2019)

8. Jones JD, Sinder BP, Paige D, Soki FN, Koh AJ, Thieleb S, **Shiozawa Y**, Hofbauer LC, Daignault S, Roca H, McCauley LK. Trabectedin reduces skeletal prostate cancer tumor size in association with effects on M2 macrophages and efferocytosis. **Neoplasia**. 2018;21:172-184. PMID: 30591422. PMCID: PMC6314218.
Status of Publication: Published
Acknowledgement of federal support: Yes

Invited reviews

(~2017)

1. **Shiozawa Y**[*], Eber MR, Berry JE, Taichman RS[*]. Bone marrow as a metastatic niche for disseminated tumor cells from solid tumors. **BoneKEy Rep**. 2015;4:689. PMID: 26029360. PMCID: PMC4440229. ([*] Co-corresponding authors)
Status of Publication: Published
Acknowledgement of federal support: Yes

2. Dai J, Hensel J, Wang N, Kruithof-de Julio M, **Shiozawa Y**. Mouse models for studying prostate cancer bone metastasis. **BoneKEy Rep**. 2016;5:777. PMID: 26916039. PMCID: PMC4757481.
Status of Publication: Published
Acknowledgement of federal support: Yes

3. Tsuzuki S, Park SH, Eber MR, Peters CM, **Shiozawa Y**. Skeletal complications in cancer patients with bone metastases. **Int J Urol**. In Press. PMID: 27488133. PMCID: In Progress.
Status of Publication: Accepted
Acknowledgement of federal support: Yes

- **The Figure 1 is chosen as the Cover Figure of Int J Urol Vol. 23 No. 10**

(2017-2018)

4. Park SH, Keller ET, **Shiozawa Y**. Bone marrow microenvironment as a regulator and therapeutic target for prostate cancer bone metastasis. **Calcif Tissue Int**. 2018;102:152-62. PMID: 29094177. PMCID: PMC5807175.
   Status of Publication: Published
   Acknowledgement of federal support: Yes

5. Widner DB, Files DC, Weaver KE, **Shiozawa Y**. Preclinical and clinical studies on cancer-associated cachexia. **Front Biol**. 2018;13:11-18. PMID: In Progress. PMCID: In Progress.
   Status of Publication: Published
   Acknowledgement of federal support: Yes

6. Park SH, Eber MR, Widner DB, **Shiozawa Y**. Role of the bone microenvironment in the development of painful complications of skeletal metastases. **Cancers (Basel)**. 2018;10:141. PMID: 29747461. PMCID: PMC5977114.
   Status of Publication: Published
   Acknowledgement of federal support: Yes

   - **Selected as Featured Paper**

7. Widner DB, Park SH, Eber MR, **Shiozawa Y**. Interactions between disseminated tumor cells and bone marrow stromal cells regulate tumor dormancy. **Curr Osteoporos Rep**. 2018;16:596-602. PMID: 30128835. PMCID: In Progress.
   Status of Publication: Published
   Acknowledgement of federal support: Yes

(2018-2019)

None.

Book

(~2017)

1. Miler SF, Thomas CY, **Shiozawa Y**. (2016) Molecular involvement of the bone marrow microenvironment in bone metastasis. In Ahmad A (Ed.), *Introduction to Cancer Metastasis.* In Press. Philadelphia, Elsevier.
   Status of Publication: Published
   Acknowledgement of federal support: Yes

(2017-2018)

2. Park SH, Eber MR, **Shiozawa Y**. (2018) Tumor inoculation mouse models of prostate cancer bone metastasis. In Idris A (Ed.), *Bone Research Protocols - 3rd Edition.* In Press. London: Springer Nature.

Status of Publication: Accepted
Acknowledgement of federal support: Yes

3. Park SH, Eber MR, Taichman RS, **Shiozawa Y**. (2018) Determining Competitive Potential of Bone Metastatic Cancer Cells in the Murine Hematopoietic Stem Cell Niche. In Turksen K (Ed.), *Stem cells and Niche - 2nd Edition: Methods and Protocols*, Methods in Molecular Biology. In Press. New York: Humana Press. Methods Mol Biol. In Press. PMID: 30099699. PMCID: In Progress.
Status of Publication: Published
Acknowledgement of federal support: Yes

(2018-2019)

None.

Presentation

(~2017)

1. Tsuzuki S, Eber MR, Miler SF, Park SH, Widner DB, **Shiozawa Y**. The effects of neuropeptides on the prostate cancer progression**.** IMPaCT Young Investigator Meeting, Baltimore, MD, USA, August 4-5, 2016. Poster.

2. Mamo M, Park SH, Eber MR, Widner DB, Tsuzuki S, Warren CC, Strickland TB, Peters CM, **Shiozawa Y**. The Interaction between Disseminated Prostate Cancer Cells and Sensory Nerves. the 2016 Annual Biomedical Research Conference for Minority Students (ABRCMS), Tampa, FL, USA, November 9-12, 2016. Poster.

(2017-2018)

3. Williams SN, Eber MR, Tsuzuki S, Park SH, **Shiozawa Y**. Does histamine influence the osteoblastic activities that help regulate the progression of bone metastatic prostate cancer? The 2017 Annual Biomedical Research Conference for Minority Students (ABRCMS), Phoenix, AZ, USA, November 1-4, 2017. Poster.

(2018-2019)

4. Lycan T, Thomas A, Hsu FC, Cartwright MS, Walker FO, Ahn C, Sangueza OP, **Shiozawa Y**, Park SH, Peters CM, Melin SA, Avery TP, Sorscher S, Lesser GJ, Strowd RE. Neuromuscular ultrasound for assessment of peripheral neuropathy in breast cancer patients receiving taxane therapy. J Clin Oncol 36, 2018 (suppl; abstr e22083). 2018 American Society Of Clinical Oncology (ASCO) Annual Meeting, Chicago, IL, USA, June 1-5, 2018. Poster.

5. Strowd RE, Lycan T, Thomas A, Hsu FC, Ahn C, Sangueza O, **Shiozawa Y**, Park SH, Peters CM, EA Romero-Sandoval, Melin SA, Sorscher S, Lesser GJ, Walker FO, Cartwright MS

Neuromuscular ultrasound for the non-invasive assessment of breast cancer patients with peripheral neuropathy from taxanes. The American Academy of Neurology 71st Annual Meeting, Philadelphia, PA, USA, May 4-10, 2019. Poster.

Website(s) or other Internet site(s)

Nothing to report.

Technologies or techniques

Nothing to report.

Inventions, patent applications, and/or licenses

Nothing to report.

Other products

Nothing to report.

7. PARTICIPANTS & OTHER COLLABORATING ORGANIZATIONS

What individuals have worked on the project?

Name: Yusuke Shiozawa
Project Role: PI
Researcher Identifier (e.g. ORCID ID): orcid.org/0000-0001-9814-9230
Nearest person month worked: 2.4
Contribution to Project: Dr. Shiozawa provides oversight of the entire program and development and implementation of all policies, procedures, and processes. In this role, Dr. Shiozawa is responsible for the implementation of the specific aims, and for ensuring that systems are in place to guarantee institutional compliance with US laws, including biosafety and animal research, data and facilities. Dr. Shiozawa supervises other personnel on the project to ensure timely and effective studies.
Funding Support: National Cancer Institution, Department of Defense

Has there been a change in the other active support of the PD/PI(s) or senior/key personnel since the last reporting period?

Nothing to report.

What other organizations have been involved as partners?

Nothing to report.

8. SPECIAL REPORTING REQUIREMENTS:

N/A.

9. APPENDICES:

The original copy of manuscript is attached.

NEOPLASIA
www.neoplasia.com

Volume 21 Number 2 February 2019 pp. 172–184 172

Trabectedin Reduces Skeletal Prostate Cancer Tumor Size in Association with Effects on M2 Macrophages and Efferocytosis[1,2]

J.D. Jones[*,3], B.P. Sinder[*,3], D. Paige[*], F.N. Soki[*], A.J. Koh[*], S. Thiele[†,‡], Y. Shiozawa[*,§], L.C. Hofbauer[†,‡], S. Daignault[¶], H. Roca[*] and L.K. McCauley[*,#]

[*]Department of Periodontics and Oral Medicine, University of Michigan School of Dentistry, Ann Arbor, MI; [†]Department of Endocrinology, Diabetes, and Bone Disease, Technische Universität Dresden Medical Center, Dresden, Germany; [‡]German Cancer Consortium (DKTK), partner site Dresden and German Cancer Research Center (DKFZ), Heidelberg, Germany; [§]Department of Cancer Biology and Comprehensive Cancer Center, Wake Forest University School of Medicine, Winston-Salem, NC; [¶]Department of Biostatistics, Center for Cancer Biostatistics, University of Michigan, Ann Arbor, MI; [#]Department of Pathology, University of Michigan Medical School, Ann Arbor, MI

Abstract

Macrophages play a dual role in regulating tumor progression. They can either reduce tumor growth by secreting antitumorigenic factors or promote tumor progression by secreting a variety of soluble factors. The purpose of this study was to define the monocyte/macrophage population prevalent in skeletal tumors, explore a mechanism employed in supporting prostate cancer (PCa) skeletal metastasis, and examine a novel therapeutic target. Phagocytic CD68+ cells were found to correlate with Gleason score in human PCa samples, and M2-like macrophages ($F4/80^+CD206^+$) were identified in PCa bone resident tumors in mice. Induced M2-like macrophages *in vitro* were more proficient at phagocytosis (efferocytosis) of apoptotic tumor cells than M1-like macrophages. Moreover, soluble factors released from efferocytic versus nonefferocytic macrophages increased PC-3 prostate cancer cell numbers *in vitro*. Trabectedin exposure reduced M2-like (F4/80+CD206+) macrophages *in vivo.* Trabectedin administration after PC-3 cell intracardiac inoculation reduced skeletal metastatic tumor growth. Preventative pretreatment with trabectedin 7 days prior to PC-3 cell injection resulted in reduced M2-like macrophages in the marrow and reduced skeletal tumor size. Together, these findings suggest that M2-like monocytes and macrophages promote PCa skeletal metastasis and that trabectedin represents a candidate therapeutic target.

Neoplasia (2019) 21, 172–184

Abbreviation: PCa, Prostate Cancer.

Address all correspondence to: Laurie K. McCauley, Department of Periodontics and Oral Medicine, University of Michigan School of Dentistry, 1101 N. University Avenue, Ann Arbor, MI 48109-1078. E-mail: mccauley@umich.edu

[1] Financial Support: This work was supported by the Department of Defense (W81XWH-14-1-0408) to Jacqueline D. Jones and Benjamin P. Sinder; Department of Defense Physician Research Training Award (W81XWH-14-1-0287) and PCF Young Investigator Award to Todd M. Morgan; Department of Defense (W81XWH-14-1-0403 and W81XWH-17-1-0541 (Y.S.)) to Yusuke Shiozawa; NIH: National Cancer Institute PO1CA093900 to Laurie K. McCauley, Yusuke Shiozawa, NIH: National Cancer Institute F32 CA168269 to Fabiana N. Soki; and Deutsche Forschungsgemeinschaft (Forschergruppe-1586 SKELMET and SPP-2084 μBONE) to S. Thiele and Lorenz C. Hofbauer.
[2] Disclosure and Conflict of Interest: L. C. H.: consultancy for Alexion, Amgen, Sandoz, Shire, Radius, and UCB.All others: no potential conflicts of interest are disclosed.
[3] Denotes co-first authors.
Received 3 April 2018; Revised 7 November 2018; Accepted 9 November 2018

1476-5586
https://doi.org/10.1016/j.neo.2018.11.003

Introduction

Bone marrow is the preferred metastatic site for prostate cancer and is rich in monocytic cells [1]. Cells of the myeloid lineage have been implicated as tumor-associated macrophages and myeloid-derived suppressor cells in the pathophysiology of various cancers [2,3]. Patients with prostate cancer (PCa) skeletal metastasis experience severe morbidity and mortality, and while macrophage targeting strategies could yield more effective therapeutic options, relatively little is known about monocytic cells in the pathophysiology of skeletal metastasis.

Monocytes and macrophages are highly heterogeneous populations with diverse subpopulations that have distinct phenotypes. A convenient paradigm for classifying macrophages is into proinflammatory "classically activated" M1-like and anti-inflammatory "alternatively activated" M2-like macrophage subtypes. Interestingly, M2-like $CD14^+CD16^+$ monocytes are elevated in the blood of cholangiocarcinoma patients, correlate with tumor-associated macrophage infiltration [4], and associate with tumor progression [4–7].

A key macrophage function is efferocytosis (phagocytosis of apoptotic cells), and macrophages are literally named for their phagocytic nature. M2-like macrophages have been positively associated with efferocytic capacity. Moreover, macrophage efferocytosis is known to induce secretion of key factors that have been implicated in tumor progression including TGF-β and CCL2 [8–10]. Indeed, previous work has demonstrated that compromised macrophage efferocytosis in MFG-E8 KO mice results in both reduced M2 polarization and prostate cancer tumor growth [9]. Therapeutic strategies to inhibit monocytes, M2-like macrophages, and efferocytosis could prove particularly beneficial to skeletal metastatic outcomes.

To explore the role of macrophages in prostate cancer skeletal metastasis and a novel treatment strategy, this study utilized the FDA-approved chemotherapeutic trabectedin (ecteinascidin 743). While trabectedin can directly inhibit certain types of cancer cells, it was recently identified to also have a highly selective and proficient ability to induce apoptosis in monocytes and macrophages [11]. In fact, trabectedin significantly reduced tumor size in cancer cells resistant to trabectedin treatment, suggesting that macrophage effects were important to its therapeutic benefit [11]. Although this demonstrated the importance of trabectedin's macrophage targeting effects, it focused solely on subcutaneous models of primary fibrosarcomas.

Given that bone marrow is the preferred metastatic site for PCa and has a unique cellular microenvironment rich in many cell types including monocytes, the present study investigated the macrophage subtypes and new treatment strategies for PCa skeletal metastasis. Specifically, two treatment strategies were explored: 1) a "preventative" treatment whereby trabectedin was administered before tumor cell inoculation to determine the impact of modulating macrophages in the bone marrow microenvironment and their role in tumor colonization of the bone microenvironment and 2) a "therapeutic" treatment regimen where trabectedin was administered after intracardiac injection of prostate cancer cells to reduce metastasis.

Materials and Methods

Cells

Luciferase-labeled PC-3 cells ($PC\text{-}3^{Luc}$) were established from the PC-3 cell line (American Type Culture Collection) as previously described [12]. $PC\text{-}3^{Luc}$ cells were regularly authenticated and matched short tandem repeat DNA profiles of the original PC-3 cell line (IDEXX Bioresearch, Westbrook, ME). Bone marrow macrophages were collected from C57BL/6J mice (Jackson laboratory, Bar Harbor) at 4-6 weeks of age for *ex vivo* and *in vitro* experiments. For *in vitro* experiments, macrophages were differentiated from bone marrow using α-MEM media with 30 ng/ml murine macrophage-colony stimulating factor (M-CSF) (eBioscience) for 6 days. At day 7, macrophages were collected and used for further analyses. For macrophage polarization, cells were treated with either IL-4 (R&D Systems) (alternatively activated-M2) or IFNγ (R&D Systems) (classically activated-M1) for 24 hours prior to efferocytosis and flow cytometric analyses. Apoptosis of PCa cells was induced by UV radiation treatment for 30 minutes followed by a 1-hour incubation at 37°C with 5% CO_2. Cells were considered highly apoptotic (HAp) if there were 70% or higher trypan blue–positive cells. Untreated tumor cells with <10% trypan blue–positive cells were considered basal apoptotic cells (BAp) as previously described [9]. Osteoclastogenesis was induced as previously described [13]. Briefly, freshly isolated bone marrow cells were treated with 30 ng/ml M-CSF and 50 ng/ml RANKL (R&D Systems). Medium was changed every 2 days. At day 7, cells were treated with or without trabectedin for 24 hours and subsequently stained for tartrate resistant acid phosphatase (TRAP) activity.

Drug

Trabectedin (PharmaMar, Colmenar Viejo, Madrid Spain) was dissolved in dimethylsulfoxide. For *in vitro* experiments, cells were treated with trabectedin (10 nM) for 24 hours. For *in vivo* experiments, mice were administered trabectedin (0.15 mg/kg/bodyweight) intravenously via tail vein injection as described [11].

Efferocytosis Assays

Bone marrow macrophages were stained with Cell Trace CSFE (Invitrogen) at 0.2 μl/ml. Fluorescently stained bone marrow cells were then co-cultured with phosphatidylserine (PS)-coated (Abcam) fluorescently labeled apoptotic mimicry beads (Bangs Laboratories, Inc.) or fluorescently tagged apoptotic PC-3 cells at a 1:3 ratio of macrophages to apoptotic bait at 37°C. Cells were washed with PBS, fixed with 10% formalin, and collected for further analysis.

Flow Cytometry

Cells (1×10^6) were resuspended in FACS buffer (PBS, 2% FBS, and 2 mM EDTA) for antibody exposure. Fluorochrome-labeled antibodies against monocyte and macrophage specific markers including F4/80 (Abcam C1:A3-1), CD86 (BioLegend GL-1), CD206 (BioLegend C068C2), CD68 (BioLegend FA-11), CD45 (BioLegend 30-F11), CD115 (BioLegend AFS98), and tumor necrosis factor receptor superfamily, member 10b (TRAILR2) (R&D Systems FAB721C) were added for 30 minutes on ice and washed three times with cold PBS. Controls included unstained samples for cell size assessment and isotype IgG control (BD Pharmingen) tagged antibodies. After antibody incubation, cells were washed twice with FACS buffer and fixed with 1% formalin. For intracellular staining, cells were subsequently permeabilized with Leucoperm (AbD Serotec) and incubated with antibodies. Data were collected and evaluated for flow cytometry analyses using BD FACSAria III and FlowJo v10 software.

RNA Extraction and Quantitative PCR

RNA isolation was performed as described previously [14] using an RNeasy mini kit (Qiagen, Valencia, CA). The cDNA

was synthesized using 0.5μg of total RNA in 50 μl of reaction volume using the TaqMan reverse transcription kit (Applied Biosystems). Quantitative real-time PCR was performed with ABI PRISM 7700 using a ready-to-use mix of primers and FAM labeled probe assay systems (Applied Biosystems) for transforming growth factor beta-1 or *Tgf-β1* (*Tgfb1*, Mm03024053_m1), chitinase-like 3 or Ym1 (*Chi3l3*, Mm00657889_mH), and tumor necrosis factor alpha-like or TNF-α (*Tnf*, Mm00443260-g1). GAPDH (*Gapdh*, Mm99999915_g1) was used as an endogenous control, and the ΔΔCT method was used to calculate the data as described previously [15].

Western Blot Analyses and Quantification

Western blot analysis and quantification were performed as previously described [9]. Primary antibodies against β-actin (1:5000, Abcam, 8227), colony stimulating factor 1 receptor (CD115) (1:1000, Abcam, 74121), and TRAILR2 (1:1000, Abcam, 8416) were used. Protein quantification was performed using the Scion Image software and calculated relative to control protein expression (β-actin).

Transwell Chemotaxis Assay for Cell Proliferation

PC-3^{Luc} cells were seeded (2.0×10^4 cells/well) onto 6-well culture plates. M-CSF expanded bone marrow–derived macrophages were loaded (1:3) into top cell culture 0.4-μm Transwell inserts (EMD Millipore) alone or with UV-induced apoptotic PC-3^{Luc} cells on day 0 and again on day 4. To measure tumor cell growth, Transwell inserts were removed, and tumor cell growth was measured using bioluminescence.

Murine Tumor Models

All animal experiments were executed under the approval and guidance of the Institutional Animal Care and Use Committees of the University of Michigan. Male athymic mice were obtained from Harlan Laboratories (Haslett, MI). For the orthotopic bone tumor model, 1×10^3 PC-3^{Luc} cells were injected into both proximal tibiae of 4- to 6-week-old athymic male mice as previously described [16]. For the experimental skeletal metastasis model, 2×10^5 PC-3^{Luc} cells were injected into the left ventricle of the heart of male athymic mice [16]. To monitor tumor growth, mice were imaged weekly via bioluminescence. After 6 weeks, animals were sacrificed and hind limbs were collected for further analysis.

Histology and Staining

After euthanasia, hind limbs were harvested and fixed with 4% paraformaldehyde/PBS at 4°C for 24 hours. Bones were then decalcified in 10% EDTA for 2 weeks and embedded in paraffin. Immunohistochemical staining was performed using a cell and tissue staining assay (HRPDAB system; R&D systems) with rabbit polyclonal antibody to CD206 (1:100; Abcam) and mouse monoclonal antibody to CD68 (1:100; Abcam). Negative controls were used to detect nonspecific staining. TRAP staining on bone sections was performed using a TRAP staining kit (Sigma-Aldrich) according to manufacturer's instructions. Staining was quantified by counting three different fields of view per specimen at 400× magnification that representatively sampled the tumor in the bone marrow. On H&E-stained sections from midtibia, bone area per tissue area was quantified in Osteomeasure software. Tissue area spanned the endocortical border and began 0.3 mm from the growth plate and extended 1 mm distally.

A human prostate cancer tissue microarray was stained for CD68 (KP1, 1:200). A representative subset of 46 patients was analyzed from a TMA containing >400 patients as previously published [17]. Assessment was carried out by one/two independent investigator/s that was/were blinded to the clinical information. The 46 patient cohort consisted of 16 benign prostatic hyperplasia (BPH), 22 Gleason ≤ 7, and 36 Gleason ≥ 8 patients. Staining was quantified by counting the sum of four different fields of view for positively stained cells at 200× magnification per specimen.

Inflammatory Cytokine Array

Serum from trabectedin-treated and control mice was collected at the end of the 6-week study. Cytokines were analyzed using the mouse inflammation antibody array C1 according to the manufacturer's instructions (AAM-INF-1-8, RayBiotech, Inc.).

Figure 1. Phagocytic CD68+ cells are positively associated with high Gleason scores, and macrophage efferocytosis supports prostate cancer cell growth. (A) Representative images of CD68 immunohistochemistry in prostate cancer tissue microarray specimens including BPH ($n=16$), Gleason ≤7 ($n=22$), and Gleason ≥8 ($n=36$). Arrowheads (black) indicate cells positive for CD68. Images are taken at 400-fold magnification. (B) Quantitative analysis of tissue specimens for the sum of CD68$^+$ cells in four different fields of view. Measured images were taken at 20× for analysis. Data are mean ± SE, *P<.05, **P<.01. (C) The association of two or more CD68$^+$ cells in tissue by patient's Gleason score was tested using Fisher's exact test. Significance was set at *P<.05. (D-E) Murine bone marrow–derived macrophages were cultured with PS-coated apoptotic mimicry beads (3:1) or fluorescently labeled apoptotic PC-3 cells (2:1) *ex vivo*, and efferocytosis was analyzed using flow cytometry for ingested beads/cells. (D) PE-labeled and unlabeled PS-coated apoptotic mimicry beads were cultured with freshly isolated bone marrow cells and analyzed by flow cytometry for F4/80$^+$ cells with ingested beads. Data are mean ± SE ($n=4$/group), *P<.05. (E) UV-induced apoptotic prostate cancer PC-3 cells (>60% high apoptosis, HAp) or noninduced PC-3 cells (<10% basal apoptosis, BAp) were cultured with freshly isolated bone marrow cells and analyzed by flow cytometry for F4/80$^+$ cells with ingested PE-labeled apoptotic tumor cells. Representative images shown with data indicated at upper right as mean ± SE ($n=4$/group), P<.05. (F-I) Pretreatment with IL4 and IFN-γ induced polarization into M1 or M2-like macrophages. (F,G) Cell surface markers F4/80, CD86, and CD206 were used to identify polarized macrophage populations using flow cytometry. Percent (%) parent population indicates the number of positive cells in the percentage of total cell population. Data are mean ± SE ($n=4$/group), #P<.0001. Representative flow cytometry images are below. (H) Relative gene expression of YM1, TGF-β, and TNF-α in polarized macrophages. Data are mean ± SE ($n=4$/group), *P<.05 vs. control. (I) Macrophage efferocytosis using fluorescently labeled HAp (PC-3) tumor cells as bait to determine the preferential behavior of polarized M1 (IFN-γ) versus M2 (IL-4) macrophages. Data are mean ± SE ($n=4$/group), *P<.05. (J) Schematic representation of experimental design to evaluate the effect of macrophages on PC-3 cell proliferation. (K) PC-3^{Luc} cells as shown in F were used to measure cell growth as a result of macrophage efferocytosis using a Transwell assay. Data are mean ± SE ($n=3$/group), *P<.05 vs. all other groups.

Statistical Analyses

Continuous outcomes are reported using means and standard errors by group. Student's *t* test was used for testing differences between two groups. Two-way ANOVA was used for two-factor experiments. Proportions of patients with two or more $CD68^+$ cells by Gleason sum were compared using Fisher's exact test. GraphPad Prism and SAS 9.3 were used for statistical analysis with a significance threshold of $P<.05$.

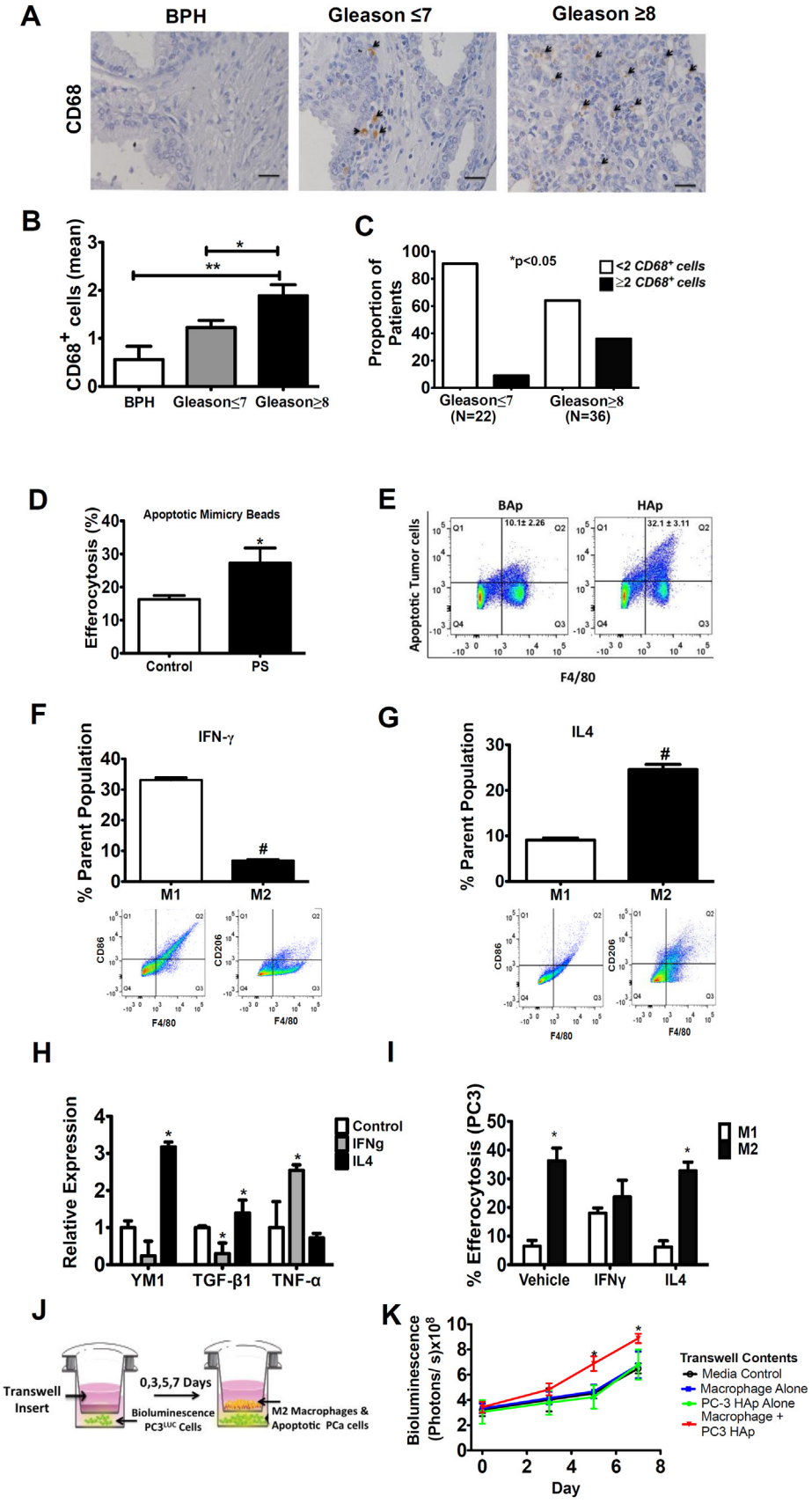

Results

Phagocytic CD68+ Cells Positively Associated with High Gleason Scores

Human prostate cancer tissue samples were first evaluated to determine the association of macrophages in the pathophysiology of prostate cancer and their potential as therapeutic targets. Monocytes were stained for CD68 expression, a scavenger receptor with an established role in phagocytosis. Samples were taken from patients characterized by BPH (n=16), Gleason score of ≤7 (n=22), and a Gleason score of ≥8 (n=36) (Figure 1*A*). Little to no expression of $CD68^+$ cells was identified in BPH specimens. Increasing numbers of CD68-positive macrophages were identified with the higher grade. Quantitative analysis of the tissue microarray revealed significantly increased numbers of $CD68^+$ cells in high-risk patients with a Gleason score ≥8 (Figure 1*B*). Further, patients with Gleason score ≥8 were more likely to have two or more $CD68^+$ cells identified compared to patients with a Gleason score ≤7 (Figure 1*C*). These data demonstrate a positive association of CD68 staining with higher-risk patients and support further exploration of macrophage and phagocytic therapeutic targets.

Prostate Cancer Cell Growth Enhanced with Macrophage Efferocytosis

The role of macrophage efferocytosis in prostate cancer cell growth was first examined with freshly isolated bone marrow cells using two different bait models (apoptotic cells or beads phagocytosed by macrophages) and analyzed using flow cytometry. Murine F4/80–positive bone marrow macrophages cultured with phosphatidylserine coated apoptotic mimicry beads displayed a significantly higher percentage of efferocytosis compared to uncoated beads (Figure 1*D*). Similarly, efferocytosis was significantly enhanced when induced highly apoptotic (HAp) PC-3 cells were incubated with F4/80 marrow macrophages compared to noninduced basal apoptotic (BAp) PC-3 cells (32.1% ± 3.1 vs. 10.1% ± 2.3) (Figure 1*E*).

Enhanced efferocytosis has been associated with cytokines that induce macrophage polarization such as IL-4 [18]. M-CSF expanded bone marrow–derived macrophages were treated with IFN-γ to induce polarization to an M1-like phenotype ($F4/80^+$, $CD86^+$), or IL-4 for an M2-like phenotype ($F4/80^+$, $CD206^+$) (Figure 1, *F*, *G*). Gene expression of TNF-α, a proinflammatory marker, was significantly increased in IFN-γ polarized macrophages. Conversely, genes associated with an anti-inflammatory response, including Ym1 and TGFβ [19,20], were significantly higher in the IL-4 polarized macrophages (Figure 1*H*).

To evaluate whether M1 or M2 macrophages are more adept at efferocytosis, HAp PC-3 cells were cultured with M1 or M2 bone marrow–derived macrophages. M2 macrophages were more proficient at efferocytosis than M1 macrophages (Figure 1*I*). Next, to evaluate the impact of efferocytosis on prostate cancer proliferation, luciferase-labeled tumor cells were incubated in a Transwell assay with macrophages undergoing efferocytosis or control macrophages as depicted in Figure 1*J*. When HAp PC3 cells were used as bait, significantly increased tumor cell growth was observed compared to all control groups (Figure 1*K*). Interestingly, the presence of macrophages alone was not sufficient to induce significant growth of tumor cells (Figure 1*K*), suggesting that the efferocytic function was required.

Single Administration of Trabectedin Reduced M2-Like Macrophages

Given the effect of M2 macrophages on efferocytosis *in vitro*, the impact of the macrophage-targeting agent trabectedin was first evaluated in the bone marrow metastatic environment without the confounding impact of a tumor as depicted in Figure 2*A*. Mice were analyzed 7 days posttreatment to ensure that the drug was completely cleared before analyzing the bone marrow and blood cellular profiles [21,22]. Trabectedin-treated mice had significantly reduced circulating $CD115^+$ blood mononuclear cells, while no significant differences were found in $CD11b^+$ or $CD45^+$ cells alone and in combination compared to vehicle control mice (Figure 2*B*). In the bone marrow microenvironment, trabectedin significantly reduced $F4/80^+$, M2-like cells ($F4/80^+$/$CD206^+$) but not M1-like cells ($F4/80^+$/$CD86^+$) (Figure 2*C*). These data suggest that M2-like cells ($F4/80^+$/$CD206^+$) macrophages and $CD115^+$ mononuclear cells are more susceptible to trabectedin treatment.

"Preventative" Trabectedin Treatment Regimen Reduces M2-Like Macrophages and Skeletal Tumor Size

Bone marrow has a high cell turnover rate, which suggests the need for phagocytic cells to engage in rapid clearance of apoptotic cells, and the presence of tumor cells in the bone can further increase the need for efferocytosis. Current work has shown that M2 polarization can be a contributing factor to tumor growth due to the release of protumorigenic factors like TGF-β, and M2-like macrophage density has been linked with tumor progression [23]. However, a defined monocyte and macrophage population in the context of PCa resident in the bone has not been fully delineated. The effect of monocyte and macrophage targeting via trabectedin was determined in an orthotopic bone prostate tumor mouse model (Figure 3*A*). A single administration of trabectedin 7 days prior to tumor inoculation resulted in decreased tumor bioluminescence in the tibiae as early as day 28 (Figure 3*B*). The mice were sacrificed at day 42 and the circulating monocytes and bone marrow cells were analyzed. Mice bearing tumors and treated with trabectedin for 6 weeks showed no differences in $CD45^+$ cells but had a trend toward an overall increase in $CD115^+$ (P=.064) cells and a significant increase in $CD11b^+$ cells (Figure 3*C*). Interestingly, in the trabectedin-treated bone marrow of resident tumor cells, a significant decrease was seen in $F4/80^+$, $CD206^+$, and $F4/80^+$/$CD206^+$ double-positive cells (Figure 3*D*). There were no differences in $CD86^+$ cells and the M1 population ($F4/80^+CD86^+$ double-positive cells) between vehicle- and trabectedin-treated mice (Figure 3*D*). The amount of bone in the tibia relative to the tissue area was not significantly different with trabectedin treatment (Suppl. Figure 3*A*). Collectively, these data show that mice treated with a single administration of trabectedin exhibited a sustained decrease in M2-like macrophages, and despite the increase in circulating $CD11b^+$ cells, this resulted in decreased tumor burden.

Reduced M2-Like Macrophages in Trabectedin-Treated, Prostate Tumor–Bearing Mice

As CD115 has been shown to be associated with resident macrophages and mature monocytes [24], the effects of trabectedin on tumor-bearing hind limbs (tibiae) were analyzed via immunohistochemistry. $CD68^+$ cells were concentrated in areas in close proximity to tumors, whereas, in trabectedin-treated mice, $CD68^+$ cell density was reduced and scattered throughout the tissue (Figure 4*A*). Although differences in $CD68^+$ cells were not identified by flow cytometric analysis of the tibia, immunohistochemistry analysis revealed a significant reduction in $CD68^+$ cells in the tissue (Figure 4*B*). $CD206^+$ cells were present in both treated and

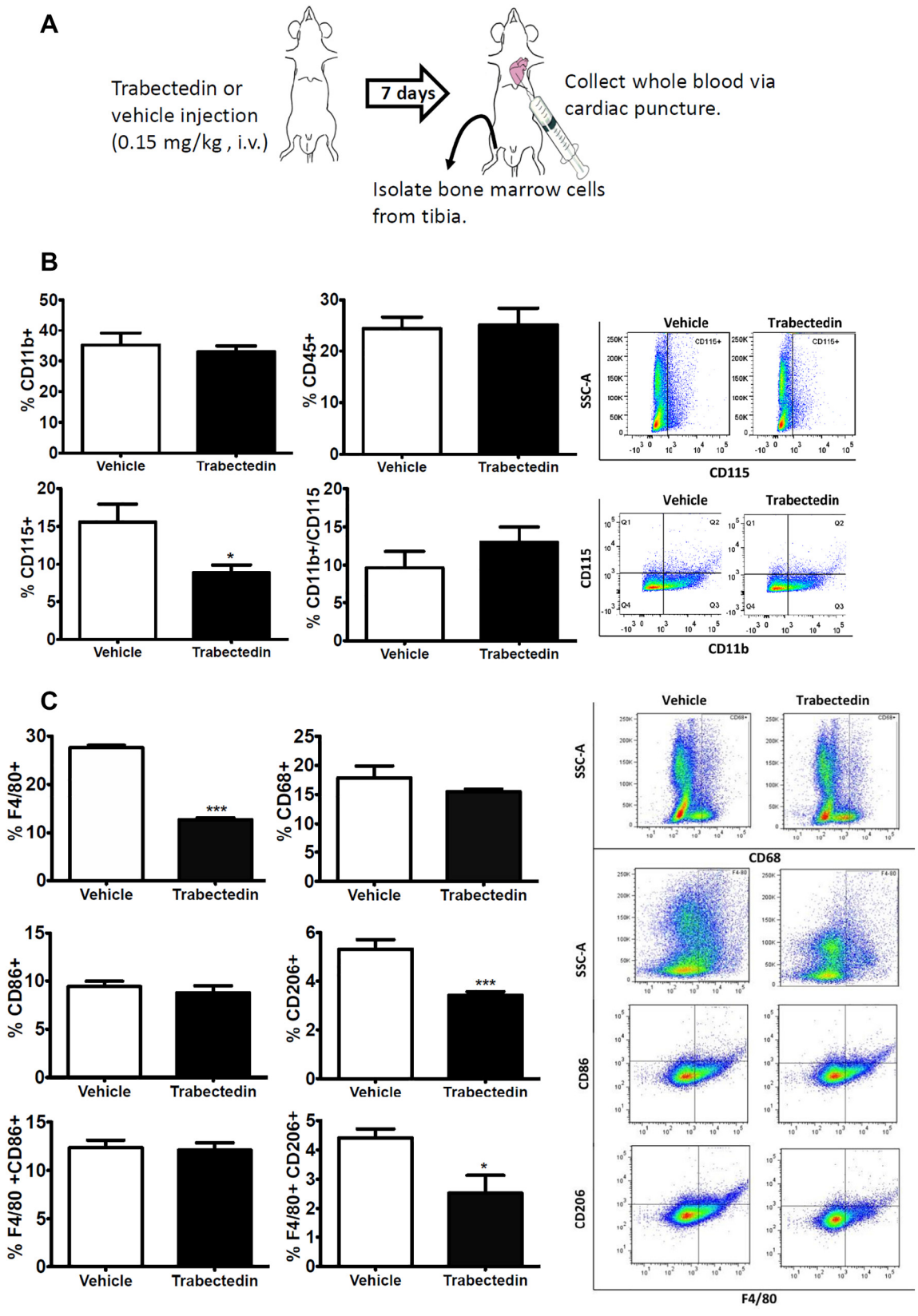

Figure 2. Single dose of trabectedin significantly reduces M2-like bone marrow cells *in vivo*. (A) Schematic representation of the experimental design. Male athymic mice were divided into two groups and treated with a single intravenous injection of saline or trabectedin (0.15 kg/mg/bodyweight). Seven days postadministration, whole blood and bone marrow cells were collected. (B) Monocytes were isolated from whole blood and flow cytometric analyses performed for $CD11b^+$, $CD45^+$, and $CD115^+$ cells. Representative flow cytometric analyses are shown. Data are mean ± SE (n=5/group), *P<.05 vs. vehicle. (C) Bone marrow cells were isolated and analyzed for markers F4/80, CD68, CD86, and CD206 using flow cytometric analyses. Representative flow cytometric analyses are shown. Data are mean ± SE (n=5/group), *P<.05, ***P<.001 vs. vehicle.

untreated mice; however, like CD68$^+$ cells in the tissue, CD206$^+$ cells appeared more dispersed throughout the tissue in treated mice (Figure 4*C*). Quantitative analysis of CD206$^+$ cells in four different areas per tibiae revealed a significant decrease in trabectedin-treated mice (Figure 4*D*). Since monocytes serve as progenitors to osteoclasts, osteoclast numbers were analyzed. Representative images of osteoclasts in the bone of tumor-bearing mice treated or untreated with trabectedin are shown in Figure 4*E*. Quantitative analysis of the number of osteoclasts was not significantly different in trabectedin-treated versus untreated mice (Figure 4*F*). These data suggest that trabectedin preferentially targeted phagocytic CD68$^+$ and CD206$^+$ cells but did not significantly decrease osteoclast number.

"Therapeutic" Trabectedin Treatment Regimen Reduces M2-Like Macrophages and Skeletal Metastasis

To investigate the effect of circulating monocytes in prostate cancer skeletal metastasis, an intracardiac skeletal metastatic tumor model for prostate cancer was utilized (Figure 5*A*) [25]. Trabectedin-treated mice presented a significant decrease in tumor bioluminescence in the hind limbs at day 35 vs. vehicle controls (Figure 5, *B-C*). Tumor bioluminescence in the mandible was significantly decreased only at day 42 (Figure 5, *B* and *D*). Interestingly, a significant decrease in F4/80$^+$, CD68$^+$, CD206$^+$, and double-positive F4/80$^+$/CD86$^+$, F4/80$^+$/CD206$^+$ cells were identified in the tibiae of trabectedin-treated mice at the end of 6 weeks (Figure 5*E*). CD11b+ cells in the blood were increased with trabectedin treatment (Suppl. Figure 2). Bone area per tissue area was reduced with trabectedin treatment (Suppl. Figure 3*B*). Trabectedin-treated mice showed a significant increase in proinflammatory cytokine levels of IL-12 ($P<.03$); soluble tumor necrosis factor receptor superfamily, member 1A (sTNFR1) ($P<.04$); chemokine (C-X-C motif) ligand 5 (LIX) ($P<.02$); and macrophage inflammatory protein-1 gamma (MIP-1γ) ($P<.01$) in the serum compared to untreated tumor-bearing mice (Supplementary Figure S1). Soluble tumor necrosis factor receptor superfamily member 1Ab (sTNFRII) levels were not significantly different ($P>.08$) in treated and untreated mice. Taken together, these data suggest that reduced tumor burden from trabectedin treatment in the clinical skeletal metastasis model may be a result of the modulation of protumorigenic mononuclear cells and proinflammatory cytokines.

Modulation of Bone Marrow–Derived Macrophages by Trabectedin

Previously, trabectedin has been shown to induce apoptosis via activation of caspase 8 by targeting TRAILR2-positive cells, which include both M1 and M2 cells [11]. In the current study, a consistent decrease in M2-like macrophages and a specific decrease in CD115 positive cells that correlated with an M2 phenotype were found. To further explore this relationship, bone marrow–derived macrophages were polarized to into M1 or M2 phenotypes *in vitro* and subsequently treated with trabectedin to determine cell numbers and the resultant levels of TRAILR2 and CD115. IL-4–treated and enriched M2 macrophages were more susceptible to trabectedin treatment than M1 macrophages *in vitro* (Figure 6*A*). There were no significant differences in the number of TRAILR2-positive cells between non–trabectedin-treated M1 and M2 populations, and both populations responded similarly to trabectedin, which suggest the presence of another potential target for trabectedin in the context of M1 vs. M2 differential responses (Figure 6*B*). As CD115 (CSF-1R) has been associated with an M2 phenotype [26–29], CD115 expression in polarized macrophage populations was analyzed using flow cytometry. IL-4–treated M2-enriched macrophages presented a significantly higher number of CD115 positive cells than IFNγ-treated M1-enriched macrophages (Figure 6*C*). There was no significant difference in TRAILR2 protein levels in M1 and M2 macrophages (Figure 6*D*). A similar trend was identified in CD115 protein levels with IL-4 treated M2 polarized macrophages (Figure 6*E*). Since monocyte/macrophages expressing both TRAILR2 and CD115 are progenitors to osteoclasts and are key effector cells in the bone, further analysis of the effect of trabectedin on osteoclasts was performed. After osteoclast expansion with RANKL (day 7), cells were treated with trabectedin for 24 hours. Osteoclasts were significantly reduced in number relative to controls (Figure 6*F*). Taken together, these results show that trabectedin targets not only TRAILR2-positive cells (M1 and M2 macrophages) but also CD115-positive cells. Moreover, a trabectedin effect on M2 macrophages may be preferential due to the increased expression of CD115 in M2, resulting in sustained suppression of M2 macrophage levels.

Discussion

Enhanced macrophage density in tumors is associated with a poor prognosis. Tumor-associated monocytes and macrophages have been shown to correlate with a protumorigenic, anti-inflammatory response [3,4,30]. Despite such findings in primary tumors, the functional role and macrophage phenotype in the context of prostate cancer skeletal metastasis have been underexplored. Macrophages are phagocytic cells that rapidly clear apoptotic debris and assist in maintaining tissue homeostasis. Our recent study reported that prostate cancer–associated macrophage efferocytosis induced an M2 polarization of macrophages *in vitro* [9]. The present study suggests that M2-like macrophage (F4/80$^+$CD206$^+$) efferocytosis is a critical cellular function which enhances prostate cancer cell growth.

Currently, there is no curative treatment for prostate cancer bone metastasis, and consequently, over 90% of patients that die from prostate cancer have bone involvement [31]. Tumor recurrence in patients having received prior chemotherapeutic treatment can be problematic due to drug effects on cells other than tumor cells in the bone/bone marrow environment. For example, cyclophosphamide, a common chemotherapeutic drug, enhanced experimental prostate cancer skeletal metastasis in association with an increase in other myeloid effector cells that supported tumor growth [25]. Interestingly, trabectedin, a novel and recently FDA-

Figure 3. Ablation of M2-like bone marrow cells retards prostate cancer tumor growth. (A) Schematic representation of the experimental design (preventative pretreatment regimen). Male athymic mice were divided into two groups and treated with a single injection of saline control ($n=10$) or trabectedin ($n=8$). Seven days after initial treatment (0.15 kg/mg/bodyweight), PC-3^{Luc} cells were injected into the bone marrow space of both the left and right tibiae, and mice were followed for 42 days. (B) Tumor growth in the hind limbs was measured weekly using bioluminescence. *$P<.05$ vs. vehicle. (C) Whole blood was collected, and monocytes were isolated and analyzed with flow cytometry for CD11b, CD45, and CD115 (with representative flow cytometric analyses). Data are mean ± SE, *$P<.05$ vs. vehicle. (D) Bone marrow cells were isolated and analyzed for markers F4/80, CD68, CD86, and CD206 using flow cytometric analysis (with representative flow cytometric analyses). Data are mean ± SE, *$P<.05$ vs. vehicle.

approved chemotherapeutic drug for the clinical treatment of sarcomas, has been shown to target phagocytic cells and induce apoptosis via caspase-8 activation [11]. While this mechanism has been approved for soft-tissue sarcomas and use in prostate cancer is being explored in clinical trials [32], the exact mechanism has not been well defined. This study showed for the first time that modulation of the bone microenvironment

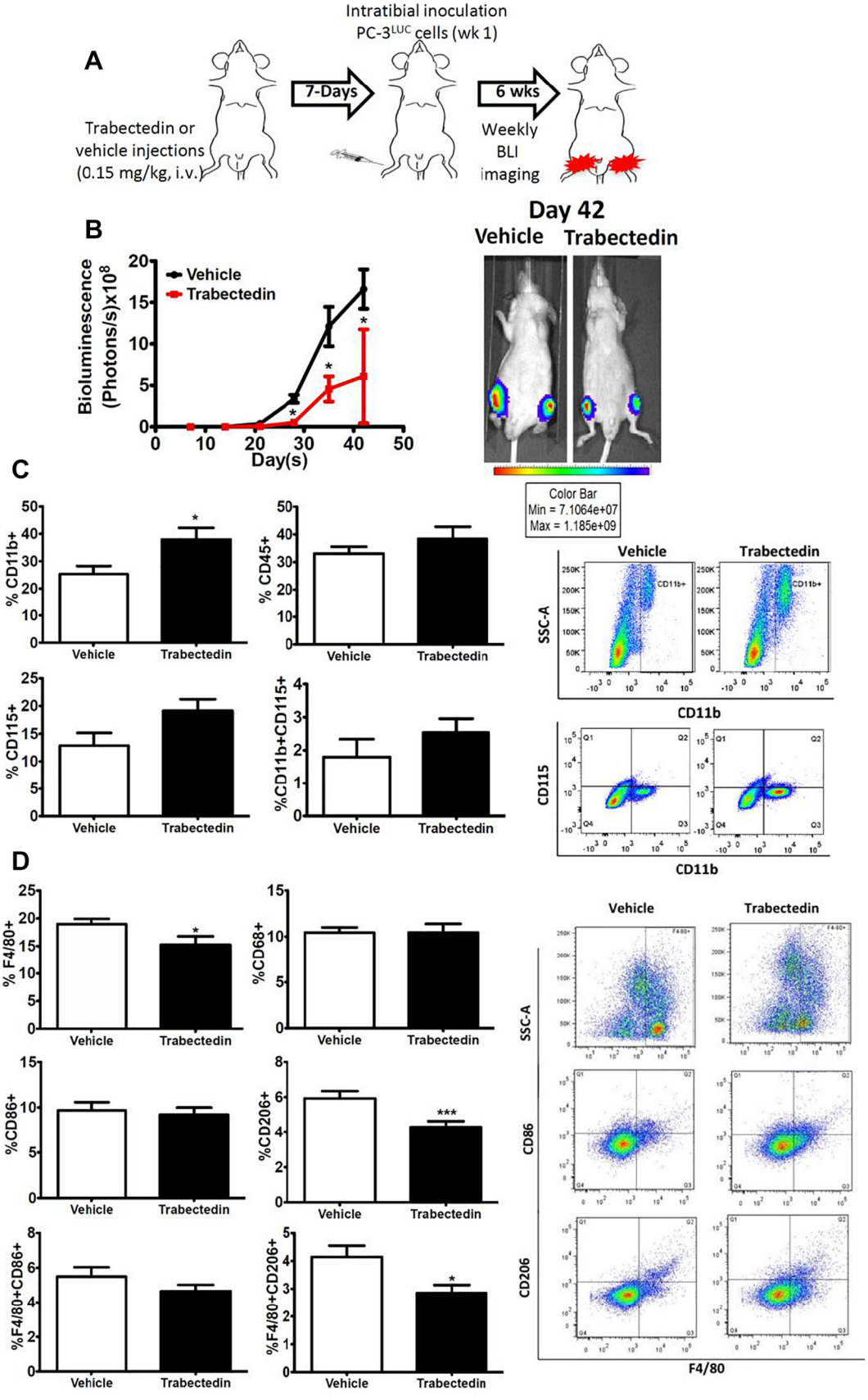

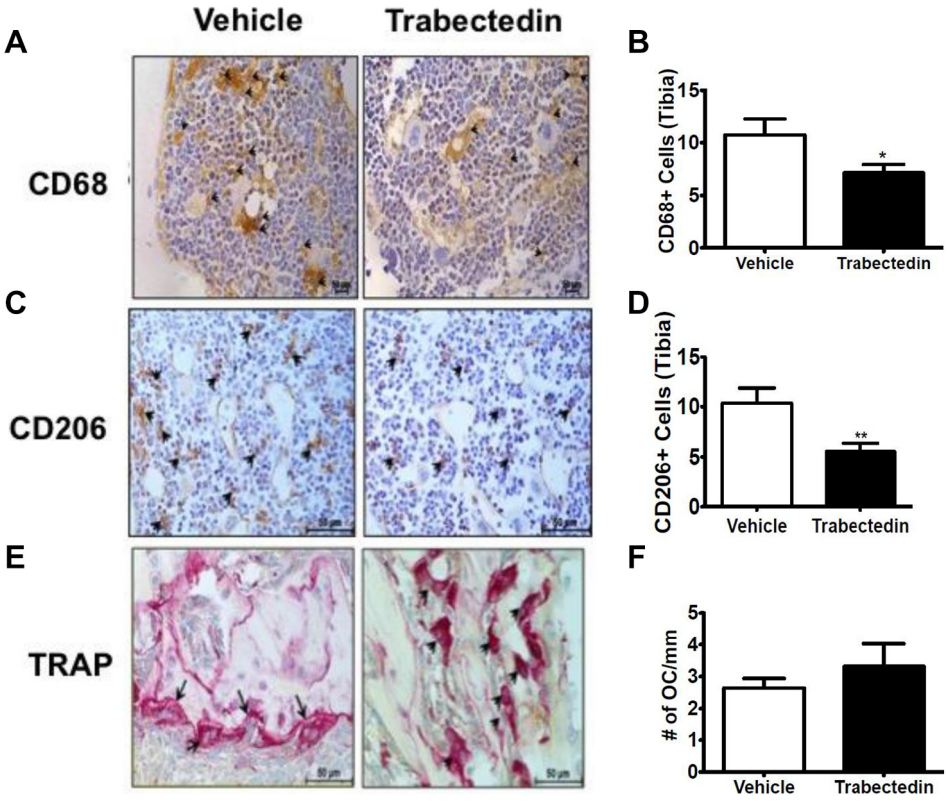

Figure 4. Immunohistochemistry of trabectedin-treated murine intratibial prostate tumors. Immunohistochemistry was performed on orthotopic tibial sections of vehicle- ($n=10$) and trabectedin- ($n=8$) treated mice as described in Figure 3. Representative images are at 400× magnification. Staining was quantified by counting three different fields of view per specimen. Arrows indicate positive cells. Data are mean ± SE. (A-B) Representative CD68 staining and quantitative analysis, *$P<.05$ vs. vehicle. (C-D) Representative CD206 staining and quantitative analysis,**$P<.01$ vs. vehicle. (E-F) Representative TRAP staining and quantification of positive osteoclastic cells (indicated by arrows) per mm of bone. There was no significant difference in osteoclast numbers.

by trabectedin preferentially reduced M2 macrophages and decreased tumor burden in the skeleton.

This study highlights both "therapeutic" and "preventative" treatment regimens which collectively highlight the importance of targeting M2-like macrophages in the bone microenvironment on PCa skeletal metastatic outcomes. In a "therapeutic" trabectedin treatment regimen, trabectedin was given biweekly *after* intracardiac injection of PC-3 cells and shown to reduce tumor size. While the reduced tumor size is likely due in part to direct effects of trabectedin on the injected PC-3 cells, it is also likely that part of the reduced tumor burden is due to inhibition of macrophages which have been previously implicated in prostate cancer metastatic outcomes [23]. Moreover, the reduced tumor size could be due to reduced prostate cancer cell growth, increased apoptosis, or both. The "preventative" trabectedin treatment regimen helps isolate the impact of bone marrow M2-like macrophages and the bone microenvironment on prostate cancer growth in the skeleton. Trabectedin, which has a half-life of under a day in rats, was given 7 days *before* PC-3 cell injection into the bone microenvironment in mice. While the M2 macrophage populations were reduced at the time point of PC-3 cell injection (7 days post-trabectedin), it is unlikely any trabectedin remained in the animal to directly inhibit newly injected cancer cells. Thus, the reduced tumor burden in the "preventative" trabectedin treatment regimen prior to cancer cell injection highlights the role of M2-like macrophages on prostate cancer metastatic growth. Targeting the M2-like macrophage populations with trabectedin or other macrophage targeting strategies may have beneficial outcomes.

The ability of trabectedin to target M2-like macrophages and their efferocytosis capabilities was shown to be a potential mechanism for prostate cancer skeletal metastatic tumor growth in this study. Specifically, it was shown that macrophage efferocytosis of cancer cells leads to secretion of factors that stimulate prostate cancer cell growth in controlled co-culture experiments, resulting in a potential positive feedback mechanism. While multiple factors are likely responsible for efferocytosis

Figure 5. M2-like monocytes and macrophages in experimental prostate cancer skeletal metastasis model. (A) Schematic of the experimental design (therapeutic treatment regimen). Male athymic mice were divided into two groups and were injected with PC-3^{Luc} in the left ventricle of the heart. Trabectedin was subsequently administered (0.15 kg/mg/bodyweight) in three doses: 7 days after tumor inoculation, at week 3, and at week 5. (B) Representative images of *in vivo* bioluminescence on day 42. (C) Hind limb metastatic tumor growth was measured by weekly *in vivo* bioluminescence imaging. Data are mean ± SE, **$P<.01$ vs. vehicle. (D) Mandibular metastatic tumor size was measured by weekly *in vivo* bioluminescence imaging. Data are mean ± SE, *$P<.05$ vs. vehicle. (E) Bone marrow cells were isolated and analyzed for markers F4/80, CD68, CD86, and CD206 using flow cytometric analysis (representative flow cytometric analyses at right). Data are mean ± SE, *$P<.05$, #$P<.0001$ vs. vehicle.

effect on prostate cancer cell growth, recent studies have identified CXCL5 as a key regulator of this response [7]. As M2-like macrophages were shown to be ~4-fold more capable of efferocytosis than M1-like macrophages in this study, inhibition of M2-like macrophages and efferocytosis by trabectedin may be particularly useful. Polarization to the M2- vs M1-like phenotype with IL4 and IFN-γ resulted in significantly

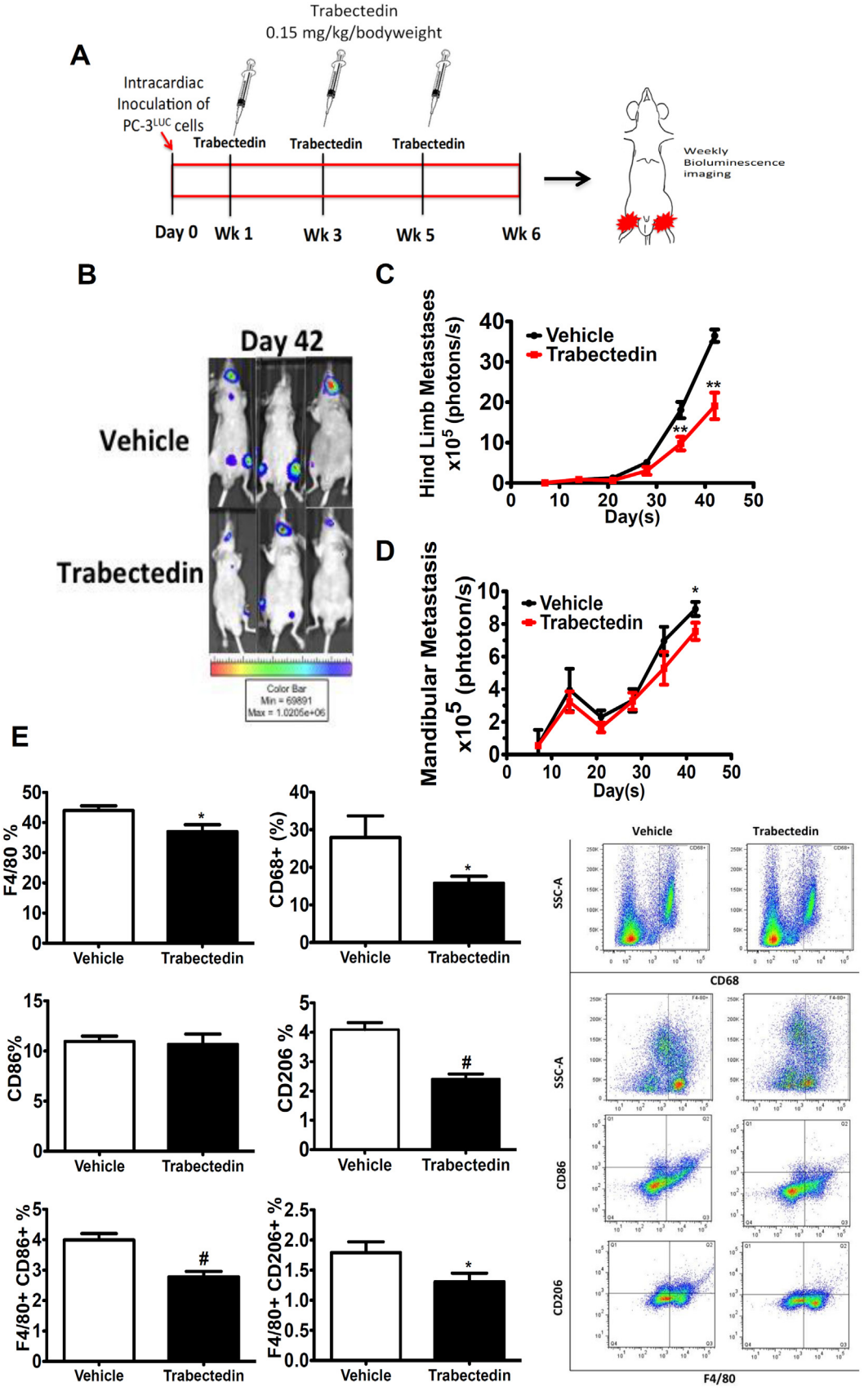

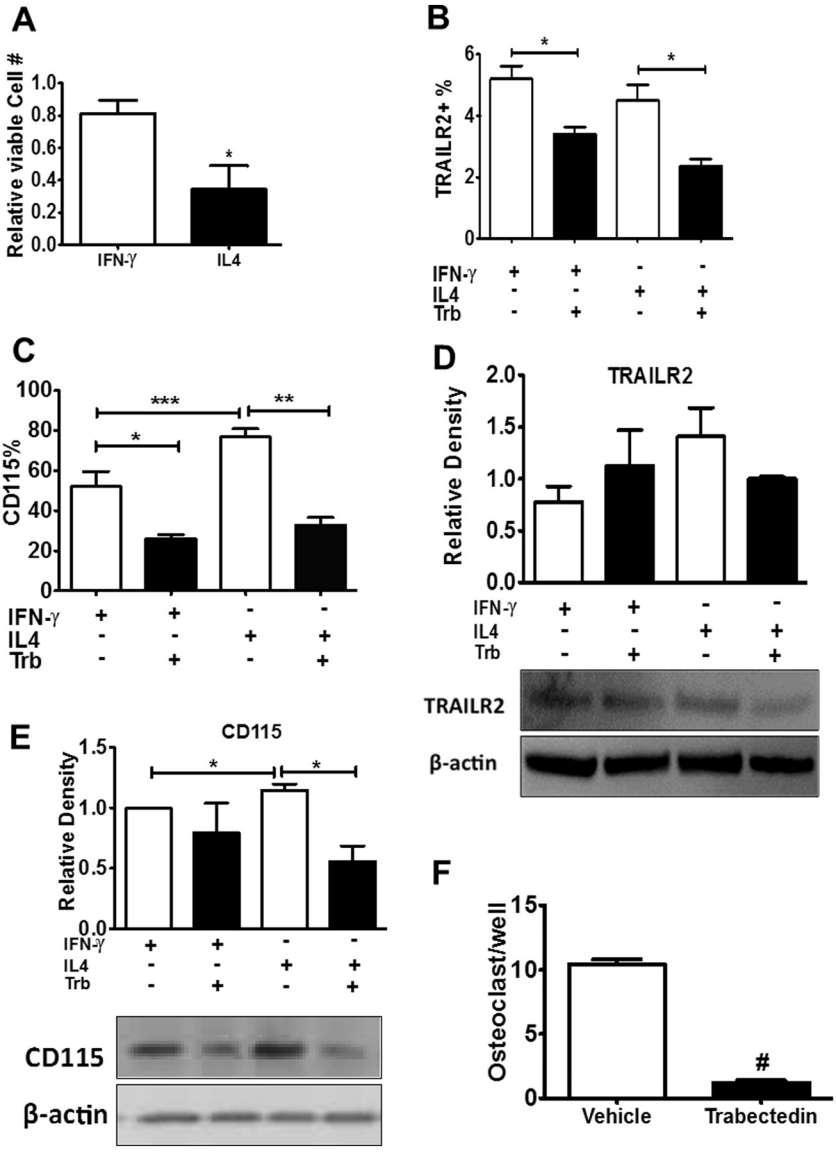

Figure 6. Modulation of polarized bone marrow–derived macrophages. (A) IL-4–treated macrophages (M2-like) were more susceptible to trabectedin treatment (10 nM) than IFN-γ treated (M1-like) *in vitro*. Viable cell numbers were normalized to untreated polarized macrophages. Data are mean ± SE (n=5/group), *P<.05. (B-C) Flow cytometric analysis of polarized macrophages untreated or treated with trabectedin *in vivo*. (B) TRAILR2$^+$; (C) CD115$^+$. Data are mean ± SE (n=4/group), *P<.05, **P<.01, ***P<.001. (D-E) Images and quantification for Western blot. (D) TRAILR2; (E) CD115. Experiments were repeated three times. Data are a mean ± SE, *P<.05. (F). Quantification of bone marrow expanded osteoclasts using RANKL, treated or untreated with trabectedin. Data are mean ± SE, #P<.0001.

greater expression of TGF-β and YM1 which are associated with a protumorigenic, anti-inflammatory response [19,20].

In this study, we observed that the phagocytic marker CD68 was positively associated with higher Gleason scores in human tumor samples, supporting a potential role of M2-like macrophages and efferocytosis in tumor growth. In humans, CD14$^+$CD16$^+$ monocytes exhibit a higher rate of phagocytosis, which is associated with acute and chronic inflammation [33]. In metastatic gastrointestinal carcinoma, patients exhibited a significant elevation in a unique CD16$^+$ monocyte population in the blood, which did not correlate with sepsis or bacterial infection [4,34]. Moreover, the presence of this monocyte subset predicted tissue invasiveness of cholangiocarcinoma and was elevated in patients with solid tumors [4,35]. Interestingly, in patients with non–small cell lung cancer, no significant difference in classical monocyte levels was found [36]. As a result, these cells tend to have a high turnover rate that may render differences more challenging to discern. In addition, patients with metastatic disease present high levels of CD115 in the blood and may recruit and stimulate polarization of macrophages to a more M2-like phenotype [37,38], further fostering an environment conducive for tumor growth. Metastatic tumor cells require CD115-positive macrophages for extravasation and growth in metastatic sites [39]. Moreover, the prostate cancer cells themselves may secrete factors such as protein kinase C zeta and MFG-E8 that may promote and M2 phenotype [9,40]. Collectively, the role of M2-like macrophages and efferocytosis is supported not only by data in this study and murine models but also by clinical observations.

Interestingly, CD11b+ cells were upregulated in the presence of a tumor with trabectedin treatment but not with trabectedin treatment

in nontumorous mice. One possibility for this discrepancy is that there is an interaction between the impact of the tumor and those of trabectedin treatment that leads to a differential effect. In addition, the trabectedin treatment history and timing are different when comparing the tumor models and to trabectedin treatment of nontumorous mice, which may also explain the observed differences.

Given the known role of trabectedin in targeting monocytes, we explored the potential effects of the agent on osteoclasts which derive from a similar lineage and contribute to prostate cancer pathophysiology [41]. Interestingly, little impact of trabectedin was observed on the number of osteoclasts *in* vivo in the tumor despite a strong *in vitro* effect on osteoclast number. The disparate *in vivo* and *in vitro* effects on osteoclasts are similar to a recent study that examined the impact of trabectedin during steady-state bone homeostasis and found no change in osteoclast surface in trabecular bone despite also identifying *in vitro* effects [42]. This may suggest that *in vivo* and around the tumor, osteoclasts are a preferentially maintained myeloid cell type.

Finally, we investigated the impact of trabectedin on bone mass in the tumor bone setting. In many bones, we observed that the primary driver of observed bone mass changes appears due to the destruction of bone by the tumor and not subtle shifts in the balance of bone remodeling. In the tibia of the direct intratibial tumor model, we found no difference in bone area per total area on histological sections with trabectedin treatment (Suppl. Figure 3*A*). In the intracardiac tumor model, we observed a significant decrease in the amount of bone in the tibia with trabectedin (Suppl. Figure 3*B*). In a prior study, we observed that, in mice without tumors, trabectedin treatment significantly reduced bone mass in the tibia [42]. The differences in bone mass between the intratibial and intracardiac tumor models could be due to several reasons. One possible explanation for this difference is that the timing and number trabectedin treatments were different between the intratibial and intracardiac models. As highlighted above, tumor itself can destroy the existing bone and may dominate any direct effects of trabectedin on the bone. Of note, the intratibial tumors are larger than the intracardiac and can lead to more bone destruction and variability than observed in the intracardiac model. Chemotherapies that directly have a negative effect on bone mass could still be beneficial to preserving bone around the tumor if they sufficiently prevent tumor growth.

In conclusion, this study showed that both "preventative" and "therapeutic" trabectedin treatment regimens are effective in preclinical models of prostate cancer. M2 (alternatively activated) monocytes and macrophages support prostate cancer skeletal metastasis, which is, in part, a result of their active engagement in efferocytosis, thus providing an anti-inflammatory environment for tumor growth. Targeting these phagocytic monocytes and macrophages with trabectedin rehabilitated the bone microenvironment by significantly decreasing M2 macrophages leading to a decrease in tumor burden. Therapies targeting these subpopulations show promise as a therapeutic approach for skeletal metastasis.

Acknowledgements

The authors thank the University of Michigan School of Dentistry histology core for assistance with histology, the University of Michigan Flow Cytometry core, Jan Berry for assistance with flow cytometry analysis, Russell Taichman for a critical read of the manuscript, and Todd Morgan and Kenneth Pienta for early feedback

Appendix A. Supplementary data

Supplementary data to this article can be found online at https://doi.org/10.1016/j.neo.2018.11.003.

References

[1] Weilbaecher KN, Guise TA, and McCauley LK (2011). Cancer to bone: a fatal attraction. *Nat Rev Cancer* **11**(6), 411–425.

[2] Sica A, Schioppa T, Mantovani A, and Allavena P (2006). Tumour-associated macrophages are a distinct M2 polarised population promoting tumour progression: potential targets of anti-cancer therapy. *Eur J Cancer* **42**(6), 717–727.

[3] Marvel D and Gabrilovich DI (2015). Myeloid-derived suppressor cells in the tumor microenvironment: expect the unexpected. *J Clin Invest* **125**(9), 3356–3364.

[4] Subimerb C, Pinlaor S, Lulitanond V, Khuntikeo N, Okada S, McGrath MS, and Wongkham S (2010). Circulating CD14+CD16+ monocyte levels predict tissue invasive character of cholangiocarcinoma. *Clin Exp Immunol* **161**(3), 471–479.

[5] Saleh MN, Goldman SJ, LoBuglio AF, Beall AC, Sabio H, McCord MC, Minasian L, Alpaugh RK, Weiner LM, and Munn DH (1995). CD16+ monocytes in patients with cancer: spontaneous elevation and pharmacologic induction by recombinant human macrophage colony-stimulating factor. *Blood* **85**(10), 2910–2917.

[6] Feng A-L, Zhu J-K, Sun J-T, Yang M-X, Neckenig MR, Wang X-W, Shao Q-Q, Song B-F, Yang Q-F, and Kong B-H, et al (2011). CD16+ monocytes in breast cancer patients: expanded by monocyte chemoattractant protein-1 and may be useful for early diagnosis. *Clin Exp Immunol* **164**(1), 57–65.

[7] Roca H, Jones JD, Purica MC, Weidner S, Koh AJ, Kuo R, Wilkinson JE, Wang Y, Daignault-Newton S, and Pienta KJ, et al (2018). Apoptosis-induced CXCL5 accelerates inflammation and growth of prostate tumor metastases in bone. *J Clin Invest* **128**(1), 248–266.

[8] Huynh M-LN, Fadok VA, and Henson PM (2002). Phosphatidylserine-dependent ingestion of apoptotic cells promotes TGF-beta1 secretion and the resolution of inflammation. *J Clin Invest* **109**(1), 41–50.

[9] Soki FN, Koh AJ, Jones JD, Kim YW, Dai J, Keller ET, Pienta KJ, Atabai K, Roca H, and McCauley LK (2014). Polarization of prostate cancer-associated macrophages is induced by milk fat globule-EGF factor 8 (MFG-E8)-mediated efferocytosis. *J Biol Chem* **289**(35), 24560–24572.

[10] Michalski MN, Koh AJ, Weidner S, Roca H, and McCauley LK (2016). Modulation of osteoblastic cell efferocytosis by bone marrow macrophages. *J Cell Biochem* **117**(12), 2697–2706.

[11] Germano G, Frapolli R, Belgiovine C, Anselmo A, Pesce S, Liguori M, Erba E, Uboldi S, Zucchetti M, and Pasqualini F, et al (2013). Role of macrophage targeting in the antitumor activity of trabectedin. *Cancer Cell* **23**(2), 249–262.

[12] Schneider A, Kalikin LM, Mattos AC, Keller ET, Allen MJ, Pienta KJ, and McCauley LK (2005). Bone turnover mediates preferential localization of prostate cancer in the skeleton. *Endocrinology* **146**(4), 1727–1736.

[13] Yamashita J, Datta NS, Chun Y-HP, Yang D-Y, Carey AA, Kreider JM, Goldstein SA, and McCauley LK (2008). Role of Bcl2 in osteoclastogenesis and PTH anabolic actions in bone. *J Bone Miner Res* **23**(5), 621–632.

[14] Koh AJ, Novince CM, Li X, Wang T, Taichman RS, and McCauley LK (2011). An irradiation-altered bone marrow microenvironment impacts anabolic actions of PTH. *Endocrinology* **152**(12), 4525–4536.

[15] Novince CM, Michalski MN, Koh AJ, Sinder BP, Entezami P, Eber MR, Pettway GJ, Rosol TJ, Wronski TJ, and Kozloff KM, et al (2012). Proteoglycan 4: a dynamic regulator of skeletogenesis and parathyroid hormone skeletal anabolism. *J Bone Miner Res* **27**(1), 11–25.

[16] Park SI, Kim SJ, McCauley LK, and Gallick GE (2010). Pre-clinical mouse models of human prostate cancer and their utility in drug discovery. *Curr Protoc Pharmacol* [Editor Board SJ Enna Ed–Chief Al, 51:14.15-14.15.27].

[17] Thiele S, Göbel A, Rachner TD, Fuessel S, Froehner M, Muders MH, Baretton GB, Bernhardt R, Jakob F, and Glüer CC, et al (2015). WNT5A has anti-prostate cancer effects in vitro and reduces tumor growth in the skeleton in vivo. *J Bone Miner Res* **30**(3), 471–480.

[18] Korns D, Frasch SC, Fernandez-Boyanapalli R, Henson PM, and Bratton DL (2011). Modulation of macrophage efferocytosis in inflammation. *Front Immunol* **2**.

[19] Raes G, De Baetselier P, Noël W, Beschin A, Brombacher F, and Hassanzadeh Gh G (2002). Differential expression of FIZZ1 and Ym1 in alternatively versus classically activated macrophages. *J Leukoc Biol* **71**(4), 597–602.

[20] Ryzhov SV, Pickup MW, Chytil A, Gorska AE, Zhang Q, Owens P, Feoktistov I, Moses HL, and Novitskiy SV (2014). Role of TGFβ signaling in generation of CD39+CD73+ myeloid cells in tumors. *J Immunol* **193**(6), 3155–3164.

[21] Perez-Ruixo JJ, Zannikos P, Hirankarn S, Stuyckens K, Ludwig EA, Soto-Matos A, Lopez-Lazaro L, and Owen JS (2007). Population pharmacokinetic meta-analysis of trabectedin (ET-743, Yondelis) in cancer patients. *Clin Pharmacokinet* **46**(10), 867–884.

[22] Reid JM, Kuffel MJ, Ruben SL, Morales JJ, Rinehart KL, Squillace DP, and Ames MM (2002). Rat and human liver cytochrome P-450 isoform metabolism of ecteinascidin 743 does not predict gender-dependent toxicity in humans. *Clin Cancer Res* **8**(9), 2952–2962.

[23] Soki FN, Cho SW, Kim YW, Jones JD, Park SI, Koh AJ, Entezami P, Daignault-Newton S, Pienta KJ, and Roca H, et al (2015). Bone marrow macrophages support prostate cancer growth in bone. *Oncotarget* **6**(34), 35782–35796.

[24] MacDonald KPA, Palmer JS, Cronau S, Seppanen E, Olver S, Raffelt NC, Kuns R, Pettit AR, Clouston A, and Wainwright B, et al (2010). An antibody against the colony-stimulating factor 1 receptor depletes the resident subset of monocytes and tissue- and tumor-associated macrophages but does not inhibit inflammation. *Blood* **116**(19), 3955–3963.

[25] Park SI, Liao J, Berry JE, Li X, Koh AJ, Michalski ME, Eber MR, Soki FN, Sadler D, and Sud S, et al (2012). Cyclophosphamide creates a receptive microenvironment for prostate cancer skeletal metastasis. *Cancer Res* **72**(10), 2522–2532.

[26] Duluc D, Delneste Y, Tan F, Moles M-P, Grimaud L, Lenoir J, Preisser L, Anegon I, Catala L, and Ifrah N, et al (2007). Tumor-associated leukemia inhibitory factor and IL-6 skew monocyte differentiation into tumor-associated macrophage-like cells. *Blood* **110**(13), 4319–4330.

[27] Haegel H, Thioudellet C, Hallet R, Geist M, Menguy T, Le Pogam F, Marchand J-B, Toh M-L, Duong V, and Calcei A, et al (2013). A unique anti-CD115 monoclonal antibody which inhibits osteolysis and skews human monocyte differentiation from M2-polarized macrophages toward dendritic cells. *MAbs* **5**(5), 736–747.

[28] Martinez MD, Schmid GJ, McKenzie JA, Ornitz DM, and Silva MJ (2010). Healing of non-displaced fractures produced by fatigue loading of the mouse ulna. *Bone* **46**(6), 1604–1612.

[29] Smith W, Feldmann M, and Londei M (1998). Human macrophages induced in vitro by macrophage colony-stimulating factor are deficient in IL-12 production. *Eur J Immunol* **28**(8), 2498–2507.

[30] Luo Y, Zhou H, Krueger J, Kaplan C, Lee S-H, Dolman C, Markowitz D, Wu W, Liu C, and Reisfeld RA, et al (2006). Targeting tumor-associated macrophages as a novel strategy against breast cancer. *J Clin Invest* **116**(8), 2132–2141.

[31] Loberg RD, Logothetis CJ, Keller ET, and Pienta KJ (2005). Pathogenesis and treatment of prostate cancer bone metastases: targeting the lethal phenotype. *J Clin Oncol* **23**(32), 8232–8241.

[32] Michaelson MD, Bellmunt J, Hudes GR, Goel S, Lee RJ, Kantoff PW, Stein CA, Lardelli P, Pardos I, and Kahatt C, et al (2012). Multicenter phase II study of trabectedin in patients with metastatic castration-resistant prostate cancer. *Ann Oncol* **23**(5), 1234–1240.

[33] Scherberich JE and Nockher WA (1999). CD14++ monocytes, CD14+/CD16+ subset and soluble CD14 as biological markers of inflammatory systemic diseases and monitoring immunosuppressive therapy. *Clin Chem Lab Med* **37**(3), 209–213.

[34] Wong KL, Tai JJ-Y, Wong W-C, Han H, Sem X, Yeap W-H, Kourilsky P, and Wong S-C (2011). Gene expression profiling reveals the defining features of the classical, intermediate, and nonclassical human monocyte subsets. *Blood* **118**(5), e16–e31.

[35] Walsh PC (2012). Re: Denosumab and bone-metastasis-free survival in men with castration-resistant prostate cancer: results of a phase 3, randomised, placebo-controlled trial. *J Urol* **187**(6), 2098.

[36] Almatroodi SA, McDonald CF, Collins AL, Darby IA, and Pouniotis DS (2014). Blood classical monocytes phenotype is not altered in primary non-small cell lung cancer. *World J Clin Oncol* **5**(5), 1078–1087.

[37] Chambers SK (2009). Role of CSF-1 in progression of epithelial ovarian cancer. *Future Oncol* **5**(9), 1429–1440.

[38] Scholl SM, Lidereau R, de la Rochefordière A, Le-Nir CC, Mosseri V, Noguès C, Pouillart P, and Stanley FR (1996). Circulating levels of the macrophage colony stimulating factor CSF-1 in primary and metastatic breast cancer patients. A pilot study. *Breast Cancer Res Treat* **39**(3), 275–283.

[39] Qian B, Deng Y, Im JH, Muschel RJ, Zou Y, Li J, Lang RA, and Pollard JW (2009). A distinct macrophage population mediates metastatic breast cancer cell extravasation, establishment and growth. *PLoS ONE* **4**(8)e6562.

[40] Fan H-H, Li L, Zhang Y-M, Yang J, Li M-C, Zeng F-Y, and Deng F (2017). PKCζ in prostate cancer cells represses the recruitment and M2 polarization of macrophages in the prostate cancer microenvironment. *Tumour Biol* **39**(6) [1010428317701442].

[41] Sinder BP, Pettit AR, and McCauley LK (2015). Macrophages: their emerging roles in bone. *J Bone Miner Res* **30**(12), 2140–2149.

[42] Sinder BP, Zweifler L, Koh AJ, Michalski MN, Hofbauer LC, Aguirre JI, Roca H, and McCauley LK (2017). Bone mass is compromised by the chemotherapeutic trabectedin in association with effects on osteoblasts and macrophage efferocytosis. *J Bone Miner Res* **32**(10), 2116–2127.